



# Drivers of CO<sub>2</sub> emissions during the dry phase of Mediterranean and Temperate ponds

Victoria Frutos-Aragón<sup>1</sup>, Sandra Brucet<sup>1,6,9</sup>, Rafael Marcé<sup>2</sup>, Tuba Bucak<sup>3</sup>, Thomas A. Davidson<sup>3</sup>,  
Louisa-Marie von Plüskow<sup>4,5</sup>, Pieter Lemmens<sup>5,7</sup>, Carolina Trochine<sup>1,8</sup>

5 <sup>1</sup> Aquatic Ecology Group, University of Vic - Central University of Catalonia, Group, Vic, 08500, Spain

<sup>2</sup> Integrative Freshwater Ecology group, Blanes Centre for Advanced Studies (CEAB-CSIC)

<sup>3</sup> Department of Ecoscience, Aarhus University, Aarhus, Denmark

<sup>4</sup> Department fish biology, Leibniz-Institute of Freshwater Ecology and Inland Fisheries, Berlin, Germany

<sup>5</sup> Laboratory of Freshwater Ecology, Evolution and Conservation, KU Leuven, Leuven, Belgium

10 <sup>6</sup> Catalan Institution for Research and Advanced Studies (ICREA), 08010 Barcelona, Spain

<sup>7</sup> Research Institute for Nature and Forest (INBO), Brussels, Belgium

<sup>8</sup> Department of Ecology, INIBIOMA CONICET, Universidad Nacional del Comahue, San Carlos de Bariloche, Argentina

<sup>9</sup> Fundació Privada Bionexus, 17003, Girona, Spain

15 *Correspondence to:* Victoria Frutos Aragón (victoriavfa@gmail.com)

**Abstract.** Pond ecosystems play an important role in the global carbon cycle with the potential to act as both sinks and sources. Emissions of CO<sub>2</sub> during their dry phases remain largely overlooked, despite growing evidence that climate change-induced shifts in temperature and precipitation will likely result in longer and more frequent dry periods. Here we assess CO<sub>2</sub> emissions from dry pond sediments in relation to climatic region, seasonal changes, and hydroperiod duration. Specifically, we aimed to identify the key environmental drivers shaping CO<sub>2</sub> fluxes during the dry phase. We measured CO<sub>2</sub> emissions from air-exposed sediments in 30 ponds across Mediterranean and Temperate regions. Ponds acted as sources of CO<sub>2</sub> during dry phases, with emissions ranging from 127 to 4889 mg C m<sup>-2</sup> d<sup>-1</sup> (mean ± SD = 1398 ± 1201). Although mean emissions did not differ significantly between climate regions, hydroperiod length interacted with climate and season, showing a significant effect in summer, particularly in Mediterranean ponds, where longer hydroperiods led to higher emissions. Emissions were considerably higher in summer than in autumn, primarily driven by an interaction between sediment temperature and water content. The highest fluxes occurred at c. 27 °C and sediment water content between 27% and 44%. Additionally, ponds in better conservation status and with lower carbonate content emitted more CO<sub>2</sub>. Our findings improve understanding of CO<sub>2</sub> emissions during increasingly common dry phases and highlight how climate modulates local sediment conditions, thereby influencing the magnitude of these emissions. This underscores the need for comprehensive assessments of carbon fluxes that incorporate dry-phase emissions, accounting for climate, hydroperiod, and both direct and indirect effects of local environmental drivers.

20  
25  
30



## 1 Introduction

Inland waters play a fundamental role in the global carbon cycle by processing substantial amounts of organic carbon from terrestrial ecosystems, that can be buried, exported, or released to the atmosphere as CO<sub>2</sub> and CH<sub>4</sub> (Cole et al., 2007; Raymond et al., 2013; Tranvik et al., 2009). Among these systems, ponds are globally abundant ecosystems that, despite covering a small portion of earth's surface, exhibit intense biogeochemical processes compared with other freshwater systems (Holgerson and Raymond, 2016; Verpoorter et al., 2014). Ponds' CO<sub>2</sub> emissions per unit area can be comparable to those of larger freshwater bodies and upland soils (Downing, 2010; Hill et al., 2021; Obrador et al., 2018; Oertli et al., 2009). One key factor influencing greenhouse gas (GHG) emissions from inland waters is drying events, which may range from partial water level reductions to complete desiccation. These events are a common feature experienced by many freshwater systems (Gao et al., 2025; Prananto et al., 2020). Globally, up to 40% of inland waters are considered non-permanent (Pickens et al., 2020), and they are particularly prevalent in arid or semi-arid regions such as the Mediterranean (Sánchez-Carrillo, 2009). The shift between wet and dry phases creates fluctuating anaerobic and aerobic conditions which affects carbon cycling, particularly CO<sub>2</sub> and CH<sub>4</sub> dynamics (Downing, 2010; Rulik et al., 2023; Zhao et al., 2020; Zou et al., 2022). As a result, CO<sub>2</sub> can dominate the total carbon emissions during dry periods while limiting CH<sub>4</sub> (Beringer et al., 2013; Zou et al., 2022). During wet phases ponds can act as either sources or sinks of atmospheric CO<sub>2</sub> having the potential to store substantial amounts of organic carbon (DeVecchia et al., 2021; Taylor et al., 2019). CO<sub>2</sub> fluxes are primarily regulated by diffusion, while its accumulation is controlled by the carbonate buffering system (Cole and Caraco, 1998). In contrast, during dry phases ponds may be sources of CO<sub>2</sub> as the absence of a water column facilitates CO<sub>2</sub> diffusion from exposed sediments, frequently resulting in increased emissions (Beringer et al., 2013; Catalán et al., 2014; Gilbert et al., 2017; Obrador et al., 2018). Global comparisons by Zou et al. (2022) and Keller et al. (2020) revealed that CO<sub>2</sub> emissions were consistently lower during the wet phases than the dry phases across temporary inland water ecosystems (streams, reservoirs, wetlands, lakes and ponds) spanning various climate regions. Particularly, ponds exhibited the highest sediment-driven emissions across inland freshwater ecosystems (Keller et al., 2020). Previous studies suggest that CO<sub>2</sub> emissions from ponds during the dry phases are largely governed by the same drivers that regulate emissions in natural soils and other aquatic environments (Håkanson, 1984; Keller et al., 2020; Martinsen et al., 2019; Oertel et al., 2016). The primary source of CO<sub>2</sub> efflux is the biological activity on organic matter in the sediments. Higher oxygen availability during dry conditions stimulates enzymatic activity and microbial degradation of organic matter by bacteria and fungi, enhancing CO<sub>2</sub> release (Fromin et al., 2010). Local factors strongly influence this process, primarily depending on sediment temperature, sediment water content and organic matter concentration (Agnew et al., 2021; Fraser et al., 2016; Jarvis et al., 2007; Lloyd and Taylor, 1994; Pozzo-Pirotta et al., 2022; Suh et al., 2009). Additionally, the composition of organic matter (e.g., humic-like components) further affects the CO<sub>2</sub> emissions (Catalán et al., 2014; Obrador et al., 2018). Other edaphic factors, such as porosity, structure, bulk density, pH, and the chemical and biological characteristics can also modulate the CO<sub>2</sub> emissions (Buragienè et al., 2019). Among biological components, macrophytes influence CO<sub>2</sub> emissions by altering sediment



65 conditions and microbial activity (Baastrup-Spohr et al., 2016; Tak et al., 2023; Weise et al., 2016). They contribute nutrients and organic compounds, including fulvic acids, which are readily decomposed by microorganisms, thereby enhancing the respiration and decomposition of organic matter (Bottino et al., 2021; Wang et al., 2017).

In addition, regional meteorological conditions, such as air temperature and precipitation, strongly influence the local and edaphic factors linked to CO<sub>2</sub> emissions, which respond sensitively to changes in sediment temperature (cold–heat) and  
70 water content (drought–excess water) (Fromin et al., 2010; Unger et al., 2010). Rewetting of previously dry soils, driven by precipitation, can trigger a rapid increase in microbial activity and subsequent CO<sub>2</sub> release, a phenomenon known as the "Birch effect" (Fromin et al., 2010; Jarvis et al., 2007). In addition, land use and conservation status can indirectly affect emissions by modifying nutrient loading sediments and the inflow of organic matter (Bartrons et al., 2025; Novikmec et al., 2016), factors known to affect emissions during the wet phase (Bhushan et al., 2024; Morant et al., 2020). However, their  
75 potential role in shaping emissions during the dry phase remains largely underexplored.

The combined effects of climate change, land-use and water abstraction, are likely to intensify the frequency and severity of drying events in regions worldwide, including central Europe and the Mediterranean region (Burkett and Kusler, 2000; Dimitriou et al., 2009; IPCC, 2014; Oroud, 2024; Pekel et al., 2016; Voudouri et al., 2023; Williams et al., 2010). In this context, it is especially concerning that the dry phases of temporary inland water bodies are often excluded in GHG studies,  
80 which tend to focus predominantly on wet periods overlooking the significant role that dry sediments can play in carbon cycling (Marcé et al., 2019). This knowledge gap likely underestimates the impact of hydrological dynamics severely limiting our understanding of the key drivers of CO<sub>2</sub> emissions during the dry phases (Hanson et al., 2015; Keller et al., 2020; Premke et al., 2016).

Here, we quantified CO<sub>2</sub> fluxes from air-exposed pond sediments during the dry phase, across different seasons (summer  
85 and/or autumn) in 30 ponds with varying hydroperiod length, located in Mediterranean and Temperate climate regions. Within this environmental and biogeochemical framework, we aimed to identify the key drivers regulating CO<sub>2</sub> emissions from dry pond sediments.

Specifically, we asked: (1) How do seasonal and climatic differences influence CO<sub>2</sub> fluxes from pond sediments during the dry phase?; (2) To what extent do climate and hydroperiod length affect CO<sub>2</sub> emissions under dry conditions?; (3) Which  
90 local sediment and environmental variables, including possible indirect factors, best explain variation in CO<sub>2</sub> fluxes across ponds?; and (4) Does macrophyte coverage, potentially reflecting conservation status, influence CO<sub>2</sub> emissions during the dry phase?.

Based on these questions, we hypothesized that:

(1) CO<sub>2</sub> fluxes from sediments during the dry phase will vary across seasons and climate regions, with higher emissions in  
95 summer due to enhanced microbial activity and organic matter decomposition; (2) climate and hydroperiod length will influence CO<sub>2</sub> emissions, with shorter hydroperiods leading to lower emissions due to reduced sediment water content and organic matter availability; (3) local sediment conditions such as temperature, sediment water content, and organic matter will primarily drive emissions, while climate sets broader seasonal and hydrological patterns; and (4) ponds with larger



macrophyte coverage, reflecting better conservation status, will exhibit greater CO<sub>2</sub> emissions due to increased vegetation senescence during the dry phase.

## 2 Methodology

### 2.1 Pond selection and data collection

We collected data from 30 ponds across four countries in Europe distributed in two climate regions, Temperate (n=14) (Belgium, Denmark and Germany) (Fig. 1a) and Mediterranean (n=16) (Spain) (Fig. 1b), spanning latitudes from 41°49'9" to 54°54'8" N and longitudes from 2°21'7" to 14° 21' 9" E.

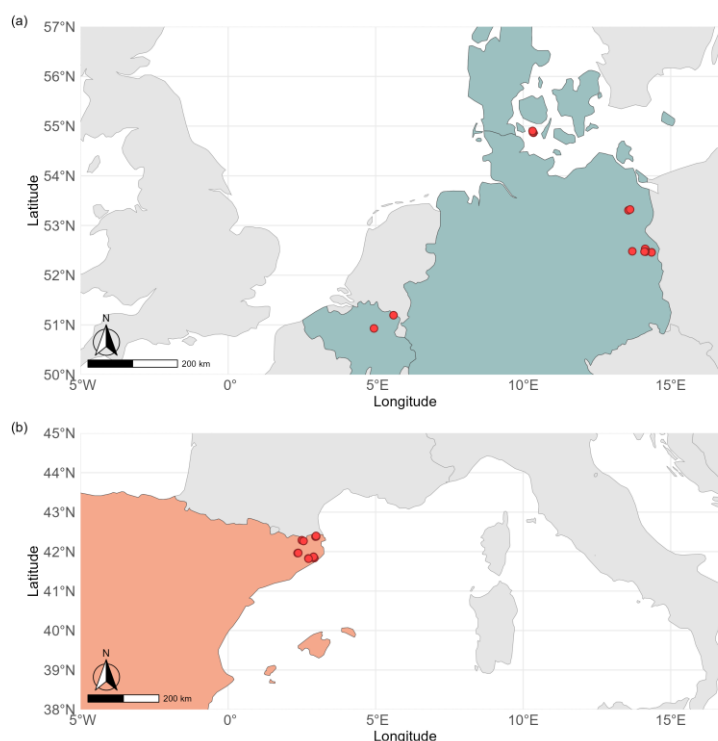


**Figure 1: Geographic location of the studied ponds. Ponds are marked with red dots. Countries are color-coded by climate region: Mediterranean (orange) and Temperate (blue).**

Our set of selected ponds included 20 temporary ponds (dry out completely every year), 5 semi-permanent ponds (dry out during some years – including the year of the sampling – but not every year) and 3 permanent ponds (never completely dry out but experienced pronounced drops in water level during the sampling year). We based this classification on hydrological information obtained from field monitoring and logger data collected between 2021 and 2023. During 2022 (the sampling year), these ponds either dried out or experienced significant water level declines, exposing large areas of the pond basin



sediments to air (on average,  $84 \pm 20\%$  of the total pond area). All ponds were located in lowland rural areas below 800 m elevation, spanning diverse land uses such as cattle-grazing lands, agricultural fields, and protected nature reserves (López-de Sancha, et al., 2025). The selected ponds covered a wide range of hydro-geomorphological and sediment characteristics (Table A1). We measured dry fluxes from bare sediment during summer ( $n=23$ ) and/or autumn ( $n=23$ ), including ponds in one or both seasons depending on the timing and extent of their water level decline.

We used a combination of regional and local factors to characterize the ponds and their surrounding landscapes, aiming to identify the main drivers of dry sediment  $\text{CO}_2$  emissions (Table A2):

## 2.2 Environmental and landscape variables

### 2.2.1 Climatic regional data

We used temperature (40-year mean of annual temperatures (1978-2018) and the annual mean for 2022) and precipitation (40-year mean annual precipitation (1978-2018) and the annual mean for 2022) calculated from the nearest cell  $1 \times 1 \text{ km}$  to each pond from the fifth generation of ECMWF atmospheric reanalysis of the global climate (ERA5) Copernicus Climate Change Service (C3S) (Wouters, 2021). We used long-term climatic averages (1978-2018) to represent the average climatic condition in the region, and the mean annual values for 2022 to capture the exceptional heat and drought conditions during the sampling year.

### 2.2.2 Hydrological data

We defined hydroperiod length as the number of months with water presence over the 12 months preceding the final sampling, which was conducted in autumn. We estimated hydroperiod length using temperature data (HOBO U2OL-0X Onset Brands) and/or water level loggers (Schlumberger Cera-Diver, accuracy  $\pm 0.02 \text{ m}$ ). The water level loggers operate based on differential pressure measurements, enabling the detection of water presence. For temperature-based assessments, we deployed two loggers: one outside the pond and another at its maximum depth. The pond was considered dry when the recorded temperatures from both sensors coincided, indicating exposure of the deepest zone. We measured pond depth profile *in situ* along two perpendicular transects at 2 m intervals using a graduated pole perpendicular to the base ground of the pond, to calculate the maximum depth. We included maximum depth in the models to assess whether this geomorphological trait (shallowness) could indirectly influence  $\text{CO}_2$  emissions under dry conditions. Pond areas were delineated through manual polygon digitization in Google Earth Pro (Google LLC, 2021), enabling georeferenced surface area calculations suitable for spatial ecological analysis.



### 2.2.3 Landscape data

We classified six land-use types: open nature, forest, pasture, arable, grassland and urban. Land use was assessed within 5 m and 100 m radii from each pond. We estimated the percentage cover of each land-use type based on visual field observations beyond these radii.

### 145 2.2.4 Conservation data

We calculated the ECELS index (Ecological Conservation of Ephemeral Lentic Systems, (Sala et al., 2005)) as a measure of pond conservation status. This index is based on five main components of the pond: pond morphology (e.g., littoral slope, burial, impermeabilization), human impacts around the pond (e.g., infrastructure, nearby land uses, rubbish), water aspects (e.g., transparency, odour), emergent vegetation (e.g., perimeter and in-pond cover, dominant community), and hydrophytic  
150 vegetation (e.g., submerged or floating vegetation). This index ranges from 0 to 100, with higher values indicating better pond conditions. In this study, we analyzed a subset of ECELS values previously reported in López-de Sancha et al. (2025a; 2025b) to assess their potential relationship with CO<sub>2</sub> emissions during the dry phase.

### 2.2.5 Water physicochemical data

We measured physicochemical parameters and Chlorophyll a during the preceding wet phase (spring) and include them as  
155 proxies for the ponds' trophic status. We determined total nitrogen (TN) and total phosphorus (TP) concentrations from unfiltered water samples (250 ml) following Sen Gupta and Koroleff, (1973). We measured dissolved organic matter (DOC) after filtering water samples through pre-combusted GF/F filters (0.7 µm pore size), using a Shimadzu TOC-L analyzer. We measured Chlorophyll a using an AlgaeTorch (bbe Moldaenke GmbH). For more detailed information, see Bartrons et al. (2025).

### 160 2.2.6 Macrophyte data

We measured macrophytes coverage *in situ* as the percentage of the pond's area covered by emerged vegetation. We also calculated macrophytes PVI (Plant Volume inhabited) as the percentage of water volume occupied by macrophytes (submerged, floating, and emergent) in the pond.

## 2.3 CO<sub>2</sub> dry fluxes measurements

165 We measured CO<sub>2</sub> emissions from the surface sediment using closed chambers in a total of 30 ponds during summer (July-August) and/or autumn (October- November) of 2022.

We equipped the closed chambers with an internal mini-logger built following Bastviken et al. (2015). We used a Sensirion SCD30 sensor module to log CO<sub>2</sub>, temperature and humidity every 2-4 seconds connecting it to an Arduino Mega250 or



Arduino one board equipped with a real-time clock and an SD card for data storage. The chamber had a small fan in the upper part to recirculate the air and therefore avoid air stratification within the chamber.

To account for the heterogeneity of the pond basin, we selected between four and eight spots in each pond, depending on its size, to measure the CO<sub>2</sub>. The chambers were fitted to a plastic collar inserted approximately 1 cm into the sediment. In each pond, we measured CO<sub>2</sub> emissions for 5-minutes at all spots except one, with a 5-minute flushing interval between measurements. At the remaining spot, we performed a 1-hour measurement. In the latter case, we additionally took manual gas samples (using a syringe and vacuum Exetainer® vials) every ten minutes. We processed these samples by gas chromatography (Agilent 8890 GC system with a PAL RSI 120 autosampler; CTC Analytics, Switzerland; (Petersen et al., 2012)).

The CO<sub>2</sub> sensors provide data in ppm units, and calibration was not required. To calculate CO<sub>2</sub> fluxes, we applied a 3-point rolling average to the raw data to reduce background noise. Flux values were then derived from the data corresponding to the last 2-3 minutes of each 5-minute measurement period, using the following Eq. (1):

$$F_{dif} = \frac{\Delta C_i}{\Delta t} * \frac{P * M}{R * T} * \frac{V_i}{A_i} * 1000 \quad (1)$$

Where  $F_{dif}$  represents the diffusive flux (mg C m<sup>-2</sup> h<sup>-1</sup>),  $\frac{\Delta C_i}{\Delta t}$  is the change in gas concentrations (ppm\* 10<sup>-6</sup>), P is the atmospheric pressure (atm), R is the gas constant (L\*atm/mol\*K), T is the temperature (K), M is the molar mass of carbon (g mol<sup>-1</sup>),  $V_i$  is the volume of the chamber (L),  $A_i$  is the area of the chamber (m<sup>2</sup>). The factor of 1000 accounts for the unit conversion from grams to milligrams.

## 2.4 Sediment characterisation

We collected sediment samples after the CO<sub>2</sub> measurement from the top 5 cm of the surface sediment layer, while temperature (°C) was taken *in situ* using a portable soil probe thermometer (TFA 30.1033 Dostmann). In the laboratory, we measured pH (HANNA Tester HI 98127) and conductivity (BiXs50 Violab conductometer), in μS cm<sup>-1</sup> at 25°C in a 1:2.5 sediment: Milli-Q mixture. Sediment water content (%) was determined as weight loss after drying 5 g of fresh homogenized sediment at 105°C furnace muffle (Carbolite Gero CWF 12/13) for 48h. The organic matter (%) and carbonate content (%) in the sediments were determined through sequential loss on ignition and expressed as percentages of the dry sediment weight. Samples were combusted in a muffle furnace (Carbolite Gero CWF 12/13) at 500 °C for 4 hours to estimate organic matter content, followed by combustion at 950 °C for 2 hours to assess mass loss associated with carbonates, commonly used as a proxy for carbonate mineral content. We assessed sediment texture using a hand-texturing method, categorized samples on the dominant material, and grouped them as clay, loamy or sandy (Thien, 1979).





#### 2.4.1 Dissolved organic matter characterization

To assess the composition of organic matter in sediments, we extracted the water-extractable organic matter (WEOM) in a 1:40 sediment water ratio (p/p) following Obrador et al. (2018). We used the solutions obtained from WEOM to determine the dissolved organic carbon (DOC) and characterized dissolved organic matter (DOM) in the sediment. We analyzed DOC using a Shimadzu TOC-VCS and expressed the results as  $\text{mg C g}^{-1}$ . We characterized DOM using absorbance and fluorescence spectroscopy to gain insights into the composition, origin, and reactivity of sedimentary organic matter. We obtained the UV-Vis absorbance spectra (200–800 nm) using a spectrophotometer (Cary 4000 UV-Vis) and fluorescence excitation-emission spectra using a fluorescence spectrophotometer HITACHI F-700. From DOM characterization, we calculated several absorbance and fluorescence indices: 1) the humification index (HIX; unitless) which indicates the degree of organic matter humification, as the ratio of the fluorescence emission peak areas between 435–480 nm and 300–345 nm at an excitation wavelength of 254 nm. 2) The biological index (BIX; unitless), which reflects the autochthonous productivity and freshness, as the ratio of the fluorescence intensities between 380 and 430 nm at an excitation wavelength of 310 nm (Fellman et al., 2010; Gabor et al., 2014; Huguet et al., 2009). 3) The fluorescence index (FI; unitless), used to assess the proportion of autochthonous versus allochthonous organic matter, as the ratio of emission intensities between 475–500 nm at an excitation wavelength of 370 nm. 4) Specific ultraviolet absorbance (SUVA;  $\text{L mg}^{-1} \text{m}^{-1}$ ), an indicator of aromaticity, calculated by dividing the UV coefficient absorbance at 254 nm by the DOC concentration ( $\text{mg/L}$ ) (Weishaar et al., 2003). 5) Absorbance at 254 nm, indicating the presence of aromatic organic compounds and used to assess the quantity and complexity of DOM. 6) Absorbance at 300 nm, reflecting the amount of less complex and more biodegradable organic compounds.

We further analyzed the DOM fluorescence properties using parallel factor analysis (PARAFAC) following Murphy et al. (2013). Multiple models were evaluated to determine the optimal number of components, based on split-half analysis validation, core consistency, model fit, and residual examination. We used the [Openfluor.org](https://openfluor.org) Platform to identify fluorescent components by matching excitation and emission spectrum to models in the repository, with a Tucker Congruence Coefficients (TCC) accuracy of 0.99 (Table S2).

We processed DOM and PARAFAC data using the R package StaRdom (Pucher et al., 2019). Further methodological details and processing steps are available in the supplementary material.

#### 2.5 Statistical analysis

We used analysis of variance (ANOVA) to compare overall  $\text{CO}_2$  emissions across climates (Mediterranean, Temperate) and seasons (Summer, Autumn) (Hypothesis 1), based on the average of multiple measurements in each pond (aov function stats package (R Core Team, 2024). To assess whether our results significantly differed from published values of pond dry fluxes, we conducted independent sample t-tests.





To investigate the influence of hydroperiod length on CO<sub>2</sub> emissions, we applied a linear mixed-effects model (LMM) (lmer function in lme4 package (Douglas Bates et al., 2015)). This model tested whether the slopes and intercepts describing the relationship between hydroperiod length and CO<sub>2</sub> emissions differed significantly between climates and seasons. Pond ID was included as random effect (Bolker et al., 2009), with CO<sub>2</sub> emissions as the response variable and hydroperiod length, season, and climate as the fixed effects. To evaluate the significance and direction of the effect of hydroperiod length within each climate and season, we extracted the estimated slopes and their 95% confidence intervals (CI) from the model (emtrends function in emmeans (Lenth, 2025)). This approach allowed us to assess how the effect (slope) of hydroperiod length on CO<sub>2</sub> emissions varied across seasons and climate regions (Hypothesis 2).

Then, to identify the main drivers of emissions across climate regions, seasons and hydroperiod (Hypothesis 3 and 4), we used Generalized Linear Mixed Models (GLMMs) using a Gaussian distribution. For these analyzes, we treated all subsamples as individual observations in the GLMMs, including Pond ID as a random intercept to account for nested data structure. We normalized all numeric variables (predictors and response) using Ordered Quantile (ORQ) normalization (orderNorm function bestNormalize package (Ryan A. Peterson, 2021)), a one-to-one transformation that transforms values into a vector that follows a Gaussian distribution (Peterson and Cavanaugh, 2020).

We assessed correlations among predictor variables (Table A2) using Pearson's correlation (Cor function in corrplot package (Wei and Simko, 2024), retaining variables with low multicollinearity ( $|r| < 0.6$ ) as fixed effects in the GLMMs. We fitted GLMMs (glmer function in lme4 package (Douglas Bates et al., 2015)), with CO<sub>2</sub> emissions as the response variable and Pond ID as a random intercept (Bolker et al., 2009). We also tested biologically relevant interactions, including the one between sediment temperature and sediment water content (Fig. S1). To capture the nonlinear relationship between sediment water content and CO<sub>2</sub> emissions, we included second-degree polynomial terms (using orthogonal polynomials) (poly function in stats package (R Core Team, 2024)) in our GLMMs (Fox, 2003). This approach allowed us to model both the linear and quadratic effects of sediment water content on CO<sub>2</sub> emissions while minimizing multicollinearity. We used multi-model inference, an automated model selection (dredge function in MuMIn package (Bartoń, 2023)) to identify the best models based on Akaike's Information Criterion (AIC) (Akaike, 1998). We calculated marginal and conditional r-squared values for the models (r.squaredGLMM function in MuMIn package (Bartoń, 2023)). We applied a four-step filtering approach to select the final models. First, we retained models in which all predictor variables were statistically significant ( $p < 0.05$ ). Second, we assessed multicollinearity using the Variance Inflation Factor (VIF) (vif function in car package (Weisberg and Fox, 2011)), ensuring that all variables included had  $VIF < 5$ . Third, we evaluated the model fit and validity using residual diagnostics (TestDispersion and testUniformity function in DHARMA package (Hartig, 2022)). This last step included assessing homoscedasticity, normality, and the absence of overdispersion or spatial autocorrelation in the residuals. Finally, we selected the model with the lowest AIC value (Akaike, 1998).

All statistical analysis were performed using R studios software (R Core Team, 2024). We used the ggplot2 R package (Wickham, 2016) to create the plots.



### 3 Results

Our study showed that ponds were overall sources of CO<sub>2</sub> to the atmosphere during the dry period, with CO<sub>2</sub> sediment emissions ranging from 127 to 4889 mg C m<sup>-2</sup> d<sup>-1</sup> (mean ± SD: 1398 ± 1201, median = 1078, n = 30). However, we also recorded some negative values indicating localized CO<sub>2</sub> uptake from the atmosphere. CO<sub>2</sub> emissions exhibited high variability both among ponds and within ponds (Fig. 2; Table 2).

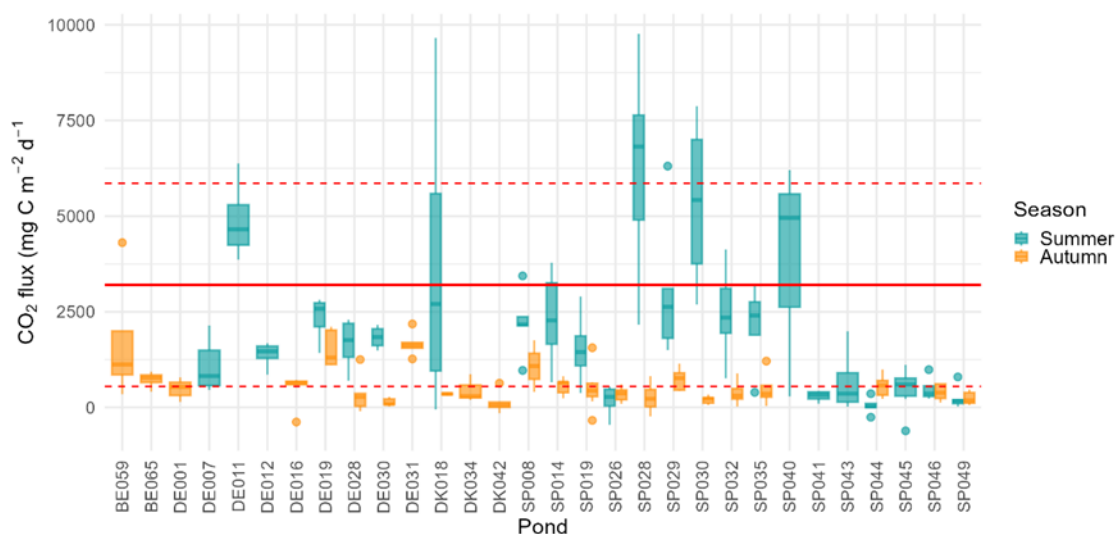


**Figure 2. Boxplots of CO<sub>2</sub> fluxes for each pond in summer and autumn. Boxes represent the interquartile range with the median indicated by a solid line; outliers are shown as individual points. The red line indicates the mean CO<sub>2</sub> flux reported by Keller et al. (2020), and the dashed lines represent the standard deviations.**



**Table 2. Summary of T-FCO<sub>2</sub> (total CO<sub>2</sub> fluxes) by season. For each pond, the table shows the mean ± standard deviation (SD) of T-FCO<sub>2</sub>, as well as the observed range (minimum to maximum) values.**

Pond	Country	Climate	Summer		Autumn	
			T-FCO <sub>2</sub> (mg C m <sup>-2</sup> d <sup>-1</sup> )	Range (Max to Min)	T-FCO <sub>2</sub> (mg C m <sup>-2</sup> d <sup>-1</sup> )	Range (Max to Min)
SP014	Spain	Mediterranean	2364 ± 1145	3779 — 663	542 ± 205	811 — 238
SP019	Spain	Mediterranean	1573 ± 757	2903 — 376	469 ± 506	1560 — -338
SP008	Spain	Mediterranean	2216 ± 878	3438 — 968	1079 ± 956	1755 — 403
SP026	Spain	Mediterranean	190 ± 383	538 — -454	346 ± 190	603 — 98
SP028	Spain	Mediterranean	6289 ± 2693	9765 — 2160	259 ± 442	817 — -234
SP029	Spain	Mediterranean	3071 ± 1919	6308 — 1501	741 ± 304	1147 — 435
SP030	Spain	Mediterranean	5356 ± 2111	7873 — 2692	198 ± 108	338 — 62
SP032	Spain	Mediterranean	2503 ± 973	4126 — 761	405 ± 283	890 — 25
SP035	Spain	Mediterranean	2133 ± 1088	3224 — 395	489 ± 504	1211 — 40
SP040	Spain	Mediterranean	3815 ± 3116	6200 to 289	-	-
SP041	Spain	Mediterranean	295 ± 148	421 to 100	-	-
SP043	Spain	Mediterranean	684 ± 899	1991 — 20	-	-
SP044	Spain	Mediterranean	46 ± 221	359 — -256	558 ± 291	991 — 228
SP045	Spain	Mediterranean	452 ± 598	1109 — -611	-	-
SP046	Spain	Mediterranean	487 ± 342	988 — 235	396 ± 220	616 — 127
SP049	Spain	Mediterranean	242 ± 280	798 — 24	243 ± 179	471 — 62
BE059	Belgium	Temperate	-	-	1726 ± 1762	4308 to 347
BE065	Belgium	Temperate	-	-	725 ± 224	937 — 414
DE001	Germany	Temperate	-	-	491 ± 248	785 — 147
DE007	Germany	Temperate	1079 ± 680	2143 — 459	-	-
DE011	Germany	Temperate	4889 ± 1085	6378 — 3866	-	-
DE012	Germany	Temperate	1391 ± 305	1677 — 857	-	-
DE016	Germany	Temperate	-	-	452 ± 468	718 — -381
DE019	Germany	Temperate	2333 ± 576	2814 — 1424	1534 ± 490	2108 — 1113
DE028	Germany	Temperate	1669 ± 634	2291 — 696	365 ± 530	1252 — -99
DE030	Germany	Temperate	1831 ± 309	2156 — 1490	136 ± 104	277 — 26
DE031	Germany	Temperate	-	-	1666 ± 332	2182 — 1268
DK018	Denmark	Temperate	3656 ± 3755	9657 — -55	353 ± 51	389 — 317
DK034	Denmark	Temperate	-	-	440 ± 281	868 — 201
DK042	Denmark	Temperate	-	-	127 ± 269	634 — -148



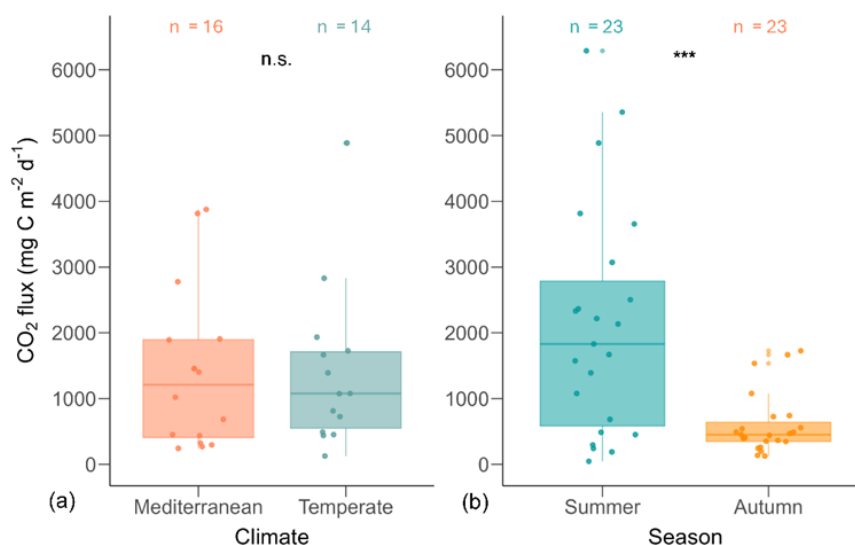
The studied ponds exhibited significant climatic and seasonal variability in their hydro-geomorphological and sediment characteristics (Table A1, S1). Mediterranean ponds exhibited higher air and sediment temperatures, shorter hydroperiods, typically drying in summer. They also showed lower sediment water content, and reduced macrophyte coverage, consistent with an earlier drying period (Table S1). In contrast, Temperate ponds had lower temperatures, longer hydroperiods and in some cases, a delayed onset of drying into autumn. These ponds also displayed higher sediment water content and macrophyte coverage (Table S1). Seasonal variation was significant only for sediment temperature ( $F_{(1,44)} = 10.64$ ,  $p < .001$ ).

Regarding sediment characteristics, the PARAFAC analysis yielded a three-component model that explained the composition of DOC. We identified the main components as: component 1 (C1), corresponding to terrestrial humic-like substances, component 2 (C2), corresponding to humic-like substances, and component 3 (C3), corresponding to tryptophan-like substances (Table S3; Fig. S7). Considering sediment composition, Mediterranean ponds exhibited lower organic matter and DOC but a higher content of C2 (humic-like), whereas Temperate ponds showed higher organic matter and DOC with a comparatively lower proportion C2 content (Table S1).

### 3.1 Climate, season, and hydroperiod variation in CO<sub>2</sub> emissions

CO<sub>2</sub> emissions from the Mediterranean ponds ranged from 242 to 3877 mg C m<sup>-2</sup> d<sup>-1</sup> (mean ± SD: 1394 ± 1207, median = 1212, n = 16), while emissions from Temperate ponds ranged from 127 to 4889 mg C m<sup>-2</sup> d<sup>-1</sup> (mean ± SD: 1403 ± 1239, median = 1078, n = 14). Fluxes did not differ between climate regions ( $F_{(1,28)} = 0$ ,  $p = .98$ ; Fig 3).

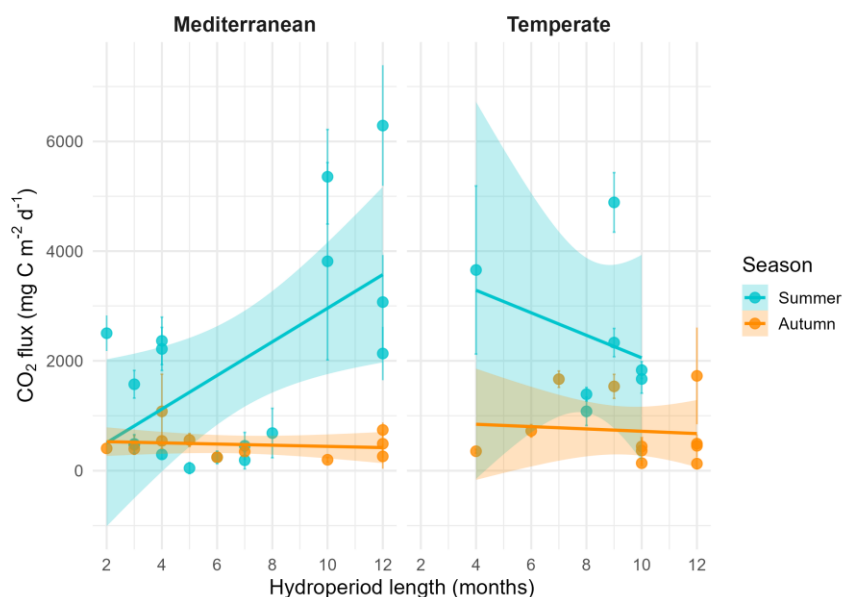
However, we found significant seasonal differences in fluxes ( $F_{(1,44)} = 16.28$ ,  $p < .001$ ; Fig. 3). During summer, fluxes ranged from 46 to 6289 mg C m<sup>-2</sup> d<sup>-1</sup> (mean ± SD: 2111 ± 1739, median: 1831, n = 23), whereas in autumn, fluxes were significantly lower, ranging from 127 to 1726 mg C m<sup>-2</sup> d<sup>-1</sup> (mean ± SD: 598 ± 464, median: 452, n = 23).





295 **Figure 3. Boxplots of CO<sub>2</sub> fluxes by climate (a) and season (b). Each point represents the mean CO<sub>2</sub> flux per pond, calculated from multiple replicate measurements. Asterisks (\*\*\*) indicate statistically significant differences based on ANOVA ( $p < 0.001$ ); NS denotes non-significant differences. The number of ponds (n) is indicated above each boxplot. Boxplot structure is described in Figure 2.**

The linear mixed-effects model (LMM) assessing the influence of hydroperiod length across season and climate regions on CO<sub>2</sub> fluxes revealed a significant three-way interaction among season, climate and hydroperiod ( $p < .01$ ). This indicates that the effect of hydroperiod was season-specific and climate-dependent (Fig. 4). Specifically, hydroperiod length significantly influenced CO<sub>2</sub> emissions only during summer in both climate regions. In Mediterranean ponds, longer hydroperiods were associated with increased CO<sub>2</sub> emissions ( $p < 0.01$ ) whereas in Temperate ponds, the trend was inverse but not statistically significant (Table 3).



305 **Figure 4. Relationship between CO<sub>2</sub> fluxes and hydroperiod length (months) by climates and seasons. Points represent individual ponds. Solid lines show linear regressions by season (blue = summer; orange = autumn) with 95% confidence intervals shaded. The dashed line represents the overall trend.**



**Table 3. Estimated slopes (effects) of hydroperiod length on CO<sub>2</sub> emissions for each combination of season (summer and autumn) and climate region (Mediterranean and Temperate). Values are derived from the linear model assessing the interaction between hydroperiod, season, and climate.**

<i>Climate</i>	<i>Season</i>	<i>Estimate</i>	<i>SE</i>	<i>df</i>	<i>lower.CL</i>	<i>upper.CL</i>
Mediterranean	Summer	290.82	78.69	27.80	129.58	452.06
Mediterranean	Autumn	17.98	81.67	31.40	-148.49	184.46
Temperate	Summer	-264.01	172.97	68.92	-609.09	81.08
Temperate	Autumn	-17.04	131.82	38.03	-283.89	249.81

We also explored the relationship between CO<sub>2</sub> fluxes and temperature (annual and 40-year mean), a variable that displayed a moderately strong inverse correlation with hydroperiod length (Fig. B1). Despite this correlation, the overall regression model encompassing emissions from all ponds, and the regressions conducted for each climate region did not yield a significant relationship ( $P > .05$ ).

### 3.2 Drivers of CO<sub>2</sub> emissions

The variables identified as potential predictors of CO<sub>2</sub> fluxes were sediment water content, sediment temperature, hydroperiod length, conservation status, coverage, PVI, pH, maximum depth, conductivity, carbonate content, DOC, BIX, HIX and SUVA which exhibited correlation coefficients ( $r$ ) predominantly between 0.6 and -0.6 (Fig. B1; B2).

We excluded absorbances at 254 and 300, FI, air temperatures (40-year and annual means), precipitation (40-year and annual means), organic matter content and components (C1, C2, C3), due to their high collinearity ( $|r| > 0.6$ ). Organic matter content exhibited a moderately strong and positive correlation with the macrophyte coverage and strong positive with DOC. Fluorescence indexes and components showed strong correlations. HIX positively correlated with terrestrial humic-like (C1) and humic-like (C2) components, and negatively with Tryptophan-like (C3) and BIX. This indicates that when organic matter is highly humified, stable, and refractory (high HIX and values), fresh, labile components, such as tryptophan-like or indicated by high BIX index, are low. Additionally, a strong negative correlation between FI and C1 suggest that higher contributions of terrestrial organic matter correspond to lower FI values, reflecting a dominant allochthonous source. Further details on organic matter components, are provided in the supplementary material (Figs. S2–S5).

Land use variables and water physicochemical variables were excluded from the final analysis due to their lack of significant association with CO<sub>2</sub> emissions during the dry phase.

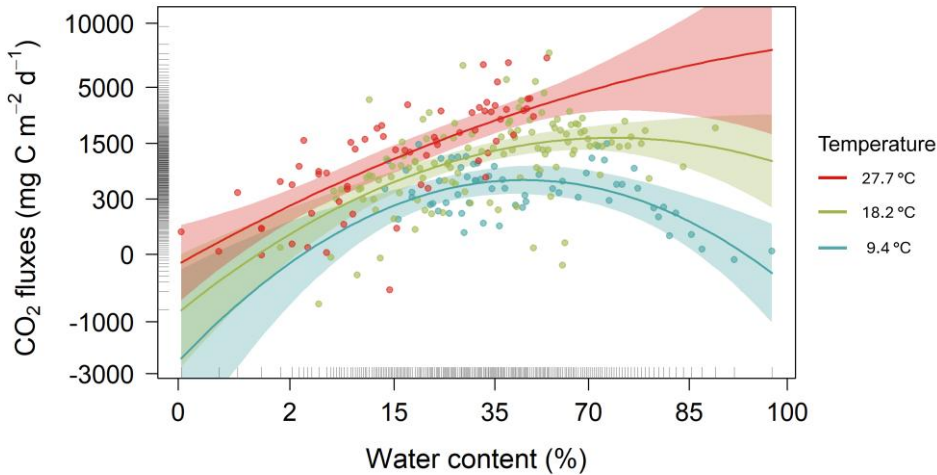
The GLMM analysis revealed significant effects of sediment water content, sediment temperature, pond conservation status, carbonate content and the interaction between sediment temperature and water content (Table 4). The model only including the interaction between sediment temperature and water content had a marginal  $R^2$  of 0.35, highlighting the importance of



these factors in explaining CO<sub>2</sub> fluxes. Additionally, incorporating the second-degree polynomial improved our model by  
335 lowering the AIC and increasing the marginal R<sup>2</sup> to 0.38, thereby better capturing the curvilinear relationship between water  
content and temperature (Fig 5). At lower temperatures (e.g., ~9.4°C), CO<sub>2</sub> emissions increased with sediment water content  
up to approximately 44%, beyond which the fluxes declined. At intermediate temperatures (~18.2°C), sediment water  
content had a moderate effect CO<sub>2</sub> fluxes. In contrast, at higher temperatures (~27.7°C), the trend reversed, and greater  
sediment water content leading to increased CO<sub>2</sub> emissions (Fig. 5). Finally, the CO<sub>2</sub> fluxes showed a positive relationship  
340 with conservation status and a negative relationship with carbonate content (Table 5).

**Table 4. Model comparison of generalized linear mixed models (GLMMs) explaining CO<sub>2</sub> emissions during the dry phase in ponds. The best model, selected based on AIC, is highlighted in bold. Temperature refers to sediment temperature.**

Model fixed effects	AIC	BIC	Deviance	Log-likelihood	Marginal R <sup>2</sup>	Conditional R <sup>2</sup>	n	df
None (null model)	684.9	695.47	678.92	-339.461	NA	0.266	249	3
Temperature	655.7	669.78	647.71	-323.85	0.123	0.429	249	4
Water content x Temperature	604.55	625.65	592.55	-296.27	0.35	0.515	249	6
(Water content + Water content <sup>2</sup> ) x Temperature	586	614.14	567	-285	0.38	0.525	249	8
(Water content + Water content <sup>2</sup> ) x Temperature+ Conservation status	583.81	615.47	565.81	-283	0.416	0.52	249	9
(Water content + Water content <sup>2</sup> ) x Temperature+ Carbonate content	581	612.9	563.27	-281.63	0.392	0.554	248	9
(Water content + Water content <sup>2</sup> ) x Temperature + Conductivity	585	619.6	567	-283.45	0.403	0.545	249	9
(Water content + Water content <sup>2</sup> ) x Temperature + Conservation status+ Conductivity	584.6	619.8	564.64	-282.32	0.431	0.545	249	10
<b>(Water content + Water content<sup>2</sup>) x Temperature+ Conservation status+ Carbonate content</b>	<b>578.43</b>	<b>613.56</b>	<b>558.43</b>	<b>-276.15</b>	<b>0.431</b>	<b>0.543</b>	<b>248</b>	<b>10</b>
(Water content + Water content <sup>2</sup> ) x Temperature + Conservation status+ Carbonate content+ Conductivity	578.76	617.41	556.76	-278.38	0.447	0.555	248	11







345 **Figure 5. Partial plot effects of the interaction between sediment water content and temperature on CO<sub>2</sub> fluxes. The figure shows results from a Generalized Linear Mixed Model (GLMM) with axes back transformed from ORQ to original scale. Each dot represents model-adjusted values, coloured lines and shaded areas depict fitted trends and 95% confidence intervals at three temperature level: blue = 9.3 °C, green = 18.2°C, and red = 27.7°C**

350 **Table 5. Results of the best Generalized Mixed Model (GLMM), including parameter estimates, explaining CO<sub>2</sub> emissions during the dry phase of the studied ponds.**

<i>Predictors</i>	<b>CO<sub>2</sub> emissions</b>		
	<i>Estimates</i>	<i>CI</i>	<i>p</i>
(Intercept)	0.07	-0.10 – 0.24	0.407
Water content [Linear]	8.32	5.54 – 11.10	<b>&lt;0.001</b>
Water content <sup>2</sup> [Quadratic]	-4.30	-6.90 – -1.70	<b>0.001</b>
Temperature	0.54	0.41 – 0.66	<b>&lt;0.001</b>
Conservation status	0.25	0.09 – 0.42	<b>0.003</b>
Carbonate content	-0.20	-0.33 – -0.08	<b>0.002</b>
Water content [Linear] x Temperature	2.69	0.33 – 5.04	<b>0.025</b>
Water content <sup>2</sup> [Quadratic] x Temperature	2.12	0.47 – 3.76	<b>0.012</b>
<b>Random Effects</b>			
$\sigma^2$	0.49		
$\tau_{00}$ Pond	0.12		
ICC	0.20		
$N_{\text{Pond}}$	30		
Observations	248		
Marginal R <sup>2</sup> / Conditional R <sup>2</sup>	0.431 / 0.543		



## 4 Discussion

Our study demonstrated that all ponds emitted CO<sub>2</sub> during the dry phase, with flux rates approximately three times higher than those reported for the wet phase of similarly sized permanent ponds (Holgerson and Raymond 2016). Seasonality strongly influenced the magnitude of emissions, with the highest fluxes observed in summer. This seasonal effect also shaped the influence of hydroperiod, which was significant only during summer and interacted with climate, leading to higher emissions in Mediterranean ponds with extended hydroperiods. The overall pattern was largely driven by the interaction between sediment temperature and water content, which followed a curvilinear relationship with a clear threshold effect. Other local factors, such as pond conservation status and carbonate content, also played a role in modulating CO<sub>2</sub> fluxes. Taken together, these findings suggest that changes in temperature, precipitation, hydroperiod, and pond ecological condition, driven by climate change, land use or other human-induced alterations, can significantly affect CO<sub>2</sub> emissions from temporary ponds.

### 4.1 CO<sub>2</sub> fluxes across ponds: influence of climate, seasonality and hydroperiod

Our study showed high variability of CO<sub>2</sub> emissions both among and within ponds, highlighting the importance of accounting for microhabitats in assessments. As hypothesized (Hypothesis 1), we found significant seasonal variation emphasizing the importance of the timing of the drying period, with the highest fluxes occurring under summer conditions. However, contrary to our expectations, overall CO<sub>2</sub> emissions did not differ significantly between climate regions (Mediterranean vs Temperate), though aligning with the findings of Keller et al. (2020) and suggesting that local factors may outweigh broader climatic influences. The CO<sub>2</sub> dry fluxes reported by Keller et al. (2020) (mean ± SD = 3204 ± 2652 mg C m<sup>-2</sup> d<sup>-1</sup> or 267 ± 221 mmol m<sup>-2</sup> d<sup>-1</sup>, n = 27), measured exclusively during the summer, were significantly higher (t-test  $p = .006$ ) than the average fluxes obtained in our study (mean ± SD = 1398 ± 1201 mg C m<sup>-2</sup> d<sup>-1</sup> or 117 ± 100 mmol m<sup>-2</sup> d<sup>-1</sup>, n = 30), which encompassed a broader seasonal range including both summer and autumn (Table 5). In contrast, there was no significant difference when comparing only summer emissions (t-test  $p = 0.15$ ). Similarly, our emission values fall within the range reported for other temporary ponds that captured different stages of the drying period (i.e., seasonal variation) (Catalán et al., 2014; DelVecchia et al., 2019; Obrador et al., 2018). This finding underscores the importance of assessing CO<sub>2</sub> emissions throughout the entire dry period, as fluxes can vary substantially over time and between seasons.



**Table 5. CO<sub>2</sub> emissions from ponds during dry and wet phases, including values from this study and previously published studies conducted across different climate regions and hydrological conditions.**

<i>Study</i>	<i>Location</i>	<i>Climate</i>	<i>CO<sub>2</sub> emissions (mg C m<sup>-2</sup> d<sup>-1</sup>)</i>	<i>Sd</i>	<i>Pond type</i>
<i>Our study</i>					
<i>Overall Ponds</i>	Europe	Temperate, Mediterranean	1398	1201	Temporary, semi-permanent, permanent
<i>Ponds in summer</i>	Europe	Temperate, Mediterranean	2111	1739	Temporary, semi-permanent, permanent
<i>Ponds in autumn</i>	Europe	Temperate, Mediterranean	598	464	Temporary, semi-permanent, permanent
<i>Inundated</i>					
<i>Holgerson and Raymond, (2016)</i>	Global (<0.001 km <sup>2</sup> )	Most general climates included	422.16	62.52	Permanent
<i>Holgerson and Raymond, (2016)</i>	Global (0.001-0.001 km <sup>2</sup> )	Most general climates included	254.52	70.56	Permanent
<i>DelVecchia et al. (2019)</i>	USA	Subalpine	128.95	123.05	Temporary, semi-permanent, permanent
<i>Dry</i>					
<i>Keller et al. (2020)</i>	Global	Tropical, temperate, polar	3204	2652	Temporary
<i>Catalan et al. (2014)</i>	Spain	Mediterranean	1455.6	1657.2	Temporary
<i>Obrador et al. (2018)</i>	Spain	Mediterranean	1293.6	1246.8	Temporary
<i>DelVecchia et al. (2019)</i>	USA	Subalpine	1813.09	320.72	Temporary, semi-permanent and permanent
<i>Martinsen et al. (2019)</i>	Sweden	Temperate	2995.2	2089.6	Not specified
<i>Fromin et al. (2010)</i>	France	Mediterranean	120-7200	n. d	Temporary
<i>DelVecchia et al. (2021)</i>	USA	Alpine	3978	138	Temporary, semi-permanent and permanent
<i>DelVecchia et al. (2021)</i>	USA	Subalpine	1713.6	541.2	Temporary, semi-permanent and permanent

This temporal variability was also reflected in the role of hydroperiod length as it showed a clear seasonal dependence, modulated by regional climate. Significant differences in emissions were observed only during summer, with contrasting trends across climate regions. Notably, the hypothesized effect of hydroperiod (Hypothesis 2) was supported only in Mediterranean ponds, where longer hydroperiods were associated with higher CO<sub>2</sub> emissions. Moreover, hydroperiod length was positively correlated with increased tryptophan-like fluorescence (C3), indicating the accumulation of less processed humic-like (C2) and more labile organic matter in the sediments (Fig. S4). The effect of both humic-like and tryptophan-like components on CO<sub>2</sub> emissions exhibited clear seasonal dependence, with significant impacts observed during summer (Fig. S5). Hydroperiod duration influences organic matter accumulation during the wet phase, which may lead to increased CO<sub>2</sub> emissions as sediments become more aerobic during the dry season (Downing, 2010; Fromin et al., 2010; Jarvis et al., 2007; Marcé et al., 2019; Obrador et al., 2018; Rulík et al., 2023). In the Mediterranean, temporary ponds are experiencing shorter hydroperiods, becoming increasingly intermittent or disappearing altogether (Gómez-Rodríguez et al., 2010). Similarly,



ponds in the Temperate region, are vulnerable to shifts from permanent to semi-permanent or temporary states (Čížková et al., 2013; Lee et al., 2015). These transitions toward more temporary systems may have important climate-warming implications, as exposed sediments can amplify CO<sub>2</sub> emissions (Marcé et al., 2019). However, our results indicate that in the Mediterranean region, climate-driven transitions toward shorter hydroperiods and more temporary pond conditions may actually reduce CO<sub>2</sub> fluxes during the dry phase. This finding highlights the need to evaluate how hydroperiods shifts impact CO<sub>2</sub> emissions across regions, considering both wet and dry phases.

#### 4.2 Drivers of CO<sub>2</sub> emissions during the dry phase

Our study identified the key drivers explaining CO<sub>2</sub> emissions from dry ponds sediments as the interaction between sediment temperature and water content, conservation status, and carbonate content. As hypothesized (Hypothesis 3), local factors, particularly the temperature-water content interaction, played a crucial role in CO<sub>2</sub> emissions from dry sediments, aligning with previous studies on dry flux emission (Keller et al., 2020; Marcé et al., 2019; Martinsen et al., 2019; Obrador et al., 2018; Oertel et al., 2016). Our results revealed a non-linear interaction between sediment water content and temperature, where water content exerts a threshold effect modulated by temperature, constraining CO<sub>2</sub> emissions at both low and high extremes of these variables. Low sediment water content limits microbial activity, reducing CO<sub>2</sub> fluxes, while saturated conditions restrict oxygen availability and gas diffusion, suppressing aerobic respiration (Almeida et al., 2019; Oertel et al., 2016; Sánchez-Carrillo, 2009). This effect is temperature-dependent, as rising temperatures stimulate microbial metabolism, and respiration, directly increasing CO<sub>2</sub> emissions (Fromin et al., 2010; Gilbert et al., 2017). Water content also influences sediment temperature, further affecting CO<sub>2</sub> fluxes (Sabater et al., 2016; Sponseller, 2007). These results highlight that sediment temperature and water content are interdependent drivers of carbon fluxes, underscoring the complex interplay between abiotic and biotic regulating these systems (Marcé et al., 2019).

In our study, dry sediment temperatures varied widely, ranging from 7 to 47.5 °C (mean ± SD: 18.8 ± 7.8 °C), with significant seasonal differences. In contrast, sediment water content did not differ significantly between seasons, although it showed a broad range from 0.89% to 94.2% (mean ± SD: 34.8 ± 24%). Our analysis predicts that CO<sub>2</sub> emissions peak at sediment temperatures around 27.7 °C and sediment water content levels between 27% to 44%. These results indicate that maximum CO<sub>2</sub> fluxes occur under intermediate sediment temperature and water content conditions, likely optimizing microbial metabolism. These findings align with Pozzo- Pirotta et al. (2022) and Gómez-Gener et al. (2016), who reported the highest emissions at temperature ranges from 18 to 25.5 °C. Conversely, temperatures exceeding ~30 °C may promote evaporation, reduce water availability and ultimately lower respiration rates due to enzyme inhibition and physiological stress (Lellei-Kovács et al., 2011). The temperature-water content relationship explains the observed seasonal pattern, with elevated temperatures enhancing microbial activity and emissions during summer, and reduced activity during autumn. Furthermore, the absence of significant differences in CO<sub>2</sub> emissions between the two climate regions may reflect the predominance of local-scale drivers, as both sediment temperature and water content conditions favourable for microbial respiration, and consequently CO<sub>2</sub> emissions, were present in ponds across both Mediterranean and Temperate climate



regions. We also found a negative relationship between CO<sub>2</sub> emissions and carbonate content, suggesting that carbonate-rich sediments may reduce mineralization rates, either by limiting microbial activity or through abiotic processes such as carbonate reactions. Although biological activity is the primary source of CO<sub>2</sub> emissions from dry sediments, abiotic processes, such as pedochemical and geological reactions (e.g., carbonate dissolution), may also contribute, albeit typically to a lesser extent (Rey, 2015). This relationship may arise because, in some regions, carbonaceous substrates modulate CO<sub>2</sub> levels during dry periods of low biological activity through weathering and precipitation reactions involving inorganic carbon (Roland et al., 2013; Hanken, Bjørlykke and Nielsen, 2015).

Moreover, as hypothesized (Hypothesis 4), ponds in better ecological condition, i.e., those with higher conservation status values, exhibited higher CO<sub>2</sub> emissions during the dry phase. Well-conserved ponds tend to support higher macrophyte diversity and vegetation cover, which enhances the accumulation and stabilization of organic carbon in sediments, promoting carbon sink during wet phases (Akasaka et al., 2010; Garcia-Murillo et al., 2025; Nag et al., 2023). In our study, pond conservation status (ECLS index) was positively correlated with both macrophyte coverage and PVI ( $P < .001$ ). In turn, macrophyte cover correlated positively with sediment organic matter and DOC ( $P < .001$ ). During dry phases, the exposure of previously vegetated sediments to air can trigger plant senescence and increase microbial activity leading to elevated CO<sub>2</sub> emissions (Catalán et al., 2014). This mechanism may help explain the counterintuitive relationship between higher conservation status and increased CO<sub>2</sub> emissions during the dry phase. Nonetheless, these higher emissions may be offset during the wet phase by lower emissions, driven by enhanced primary production and greater carbon burial (Page and Dalal, 2011; Morant et al., 2020; Zou et al., 2022). It is important to note that our CO<sub>2</sub> flux measurements were taken from bare sediment and do not account for the effects of primary production and net ecosystem metabolism, suggesting that the overall fluxes from these systems are likely lower than indicated here. Finally, conservation status, represented by the ECLS index, which integrates pond morphology, human impacts, vegetation abundance, and water quality, appears to be a stronger predictor of CO<sub>2</sub> emissions during the dry phase than individual factors such as land use or trophic status proxies (e.g., Chlorophyll a, TN, TP). This highlights the value of integrative ecological indices over isolated proxies when evaluating pond function.

### 4.3 Implications of our study in the context of global change

Overall, our results emphasize the importance of assessing CO<sub>2</sub> emissions throughout the entire dry period, as key drivers such as sediment temperature and water content can fluctuate over short time scales and are strongly influenced by climatic conditions. Capturing this temporal variability is critical, as single-time-point measurements may underestimate the actual emissions dynamics of these ecosystems. Incorporating this variability into carbon budgets will improve their accuracy and enhance the design of climate mitigation strategies that consider CO<sub>2</sub> emissions from dry sediments. Despite their relevance, studies quantifying CO<sub>2</sub> fluxes during dry phases remain scarce, creating a critical knowledge gap that limits the inclusion of temporary systems into global GHG inventories (Keller et al., 2020; Lauerwald et al., 2023; Marcé et al., 2019).



Our findings also suggest that projected increases in temperature are likely to elevate sediment temperatures, which, especially when combined with episodic rewetting events, may substantially enhance CO<sub>2</sub> emissions during dry phases. In addition, ponds with more permanent hydroperiods exhibited higher dry-phase CO<sub>2</sub> fluxes than ephemeral systems in Mediterranean regions. However, to fully understand how shifts in hydroperiod toward increased intermittency affect carbon dynamics, future studies should integrate measurements from both wet and dry phases.

Understanding these processes is essential in the context of climate change, as climate regions are facing divergent hydrologic trends (Pekel et al., 2016; Wang et al., 2018; Vicente-Serrano et al., 2022; Bevacqua et al., 2024). Given that extreme events, such as the severe 2022 European drought (Copernicus Climate Change Service (C3S), 2023), are expected to become more frequent, and that anthropogenic pressures continue to intensify, inland water systems are undergoing rapid transformations that will increasingly influence the global carbon cycle.



## Appendix A: hydro-geomorphological and sediment characteristics

**Table A1. Hydro-geomorphological and sediment characteristic of the studied ponds.**

<i>Pond</i>	<i>Longitude</i>	<i>Latitude</i>	<i>Country</i>	<i>Climate</i>	<i>Area (m<sup>2</sup>)</i>	<i>Maximum depth (cm)</i>	<i>Hydroperiod length (Months)</i>	<i>Season</i>	<i>Temperature (°C)</i>	<i>Water content (%)</i>	<i>pH</i>	<i>Conductivity (μS/cm)</i>	<i>Carbonate content (%)</i>	<i>Organic matter (%)</i>	<i>DOC (mg C/g)</i>
<i>SP008</i>	2.98	42.4	Spain	Mediterranean	2555.36	127	4	Summer	24.94	12.80	4.99	314.6	0.73	16.01	2.36
								Autumn	18.2	19.51	4.93	420.4	1.25	12.52	1.17
<i>SP014</i>	2.96	42.38	Spain	Mediterranean	13465.72	121	4	Summer	22.27	29.87	4.91	595.71	1.44	23.69	1.18
								Autumn	16.44	19.07	4.77	786	1.76	23.77	1.77
<i>SP019</i>	2.98	42.38	Spain	Mediterranean	11455.29	125	3	Summer	25.4	19.40	5.08	389.22	0.94	17.08	1.66
								Autumn	14.66	14.32	5.05	456.22	1.34	17.68	1.52
<i>SP026</i>	2.35	41.96	Spain	Mediterranean	176.62	77	7	Summer	20.15	3.59	7.53	957.5	0.15	2.78	0.39
								Autumn	10.43	27.95	7.47	459.67	22.53	4.33	0.4
<i>SP028</i>	2.36	41.96	Spain	Mediterranean	324.84	104	12	Summer	18.83	32.39	7.2	718.17	0.22	5.85	0.48
								Autumn	12.25	41.30	7.2	318	19.72	8.74	0.62
<i>SP029</i>	2.37	41.97	Spain	Mediterranean	128.52	140	12	Summer	26.74	39.30	7.24	422.6	3.52	16.78	0.56
								Autumn	10.98	30.93	7.38	334.8	18.95	5.21	0.48
<i>SP030</i>	2.38	41.96	Spain	Mediterranean	248.35	137	10	Summer	25.83	38.78	7.22	556.33	0.21	5.39	0.74
								Autumn	11.42	38.39	7.26	325.83	18.39	5.7	0.56
<i>SP032</i>	2.72	41.83	Spain	Mediterranean	565.29	146	2	Summer	25.98	31.87	7.3	713.22	0.52	6.23	0.38
								Autumn	9.29	24.47	7.52	336.22	1.46	6.26	0.47
<i>SP035</i>	2.72	41.82	Spain	Mediterranean	307.7	118	12	Summer	27.82	38.32	6.97	244.34	0.1	6.17	0.63
								Autumn	12.68	29.42	6.84	134.88	0.69	4.4	0.5
<i>SP040</i>	2.5	42.28	Spain	Mediterranean	86.05	85	10	Summer	26.98	43.65	7.39	480.25	20.91	7.15	1.32
<i>SP041</i>	2.5	42.29	Spain	Mediterranean	84.39	72	4	Summer	27.36	2.51	7.76	282.8	5.31	10.37	1.47
<i>SP043</i>	2.56	42.27	Spain	Mediterranean	157.48	58	8	Summer	39.33	2.15	7.67	462.5	21.84	14.33	1.92
<i>SP044</i>	2.92	41.84	Spain	Mediterranean	1205.68	93	5	Summer	33.17	3.63	7.39	628.33	0.89	11.71	0.83
								Autumn	15.03	33.91	7.84	245.83	8.52	12.37	1.23
<i>SP045</i>	2.88	41.84	Spain	Mediterranean	65.42	148	7	Summer	26.77	13.49	6.38	131.33	0.44	1.78	0.33
<i>SP046</i>	2.9	41.87	Spain	Mediterranean	504.42	72	3	Summer	32.76	5.02	5.61	106.64	0.13	15.28	4.6
								Autumn	8.56	20.16	5.61	106.64	0.8	3.99	0.63
<i>SP049</i>	2.89	41.87	Spain	Mediterranean	99.4	73	6	Summer	32	3.97	6.11	147.22	1.3	7.69	0.46
								Autumn	9.08	20.56	5.87	96.52	0.83	2.27	0.29
<i>BE059</i>	4.94	50.93	Belgium	Temperate	98	87	12	Autumn	16.33	21.04	6.11	485.53	0.73	5.08	0.64
<i>BE065</i>	5.61	51.19	Belgium	Temperate	380	83.75	6	Autumn	16.55	9.31	6.17	59.83	0.33	1.15	0.3
<i>DE001</i>	14.11	52.47	Germany	Temperate	2250	262	12	Autumn	12.3	80.96	7.25	453.67	1.54	46.89	7.67
<i>DE007</i>	13.7	52.48	Germany	Temperate	1350	170	8	Summer	19.99	63.59	6.73	305.33	1.08	32.2	2.04
<i>DE011</i>	14.35	52.46	Germany	Temperate	1500	83	9	Summer	21.5	66.37	7.35	457.83	14.8	20.75	2.33
<i>DE012</i>	14.35	52.46	Germany	Temperate	2800	69	8	Summer	19.95	68.92	7.57	1484.5	13.41	21.93	2.15
<i>DE016</i>	13.62	53.32	Germany	Temperate	150	160	12	Autumn	13.8	61.11	6.96	462.2	2.12	11.32	1.8
<i>DE019</i>	13.57	53.31	Germany	Temperate	60	70	9	Summer	19.7	41.15	5.61	615	2.28	12.53	1.28
<i>DE028</i>	14.14	52.47	Germany	Temperate	600	115	10	Summer	24.64	23.06	6.65	741	1.59	8.16	0.79
								Autumn	13.52	19.46	6.29	1504.8	1.39	7.26	1.52
<i>DE030</i>	14.14	52.52	Germany	Temperate	1200	55	10	Summer	23.81	75.01	7.12	581.2	2.04	33.58	1.89
								Autumn	10.83	79.48	6.77	450.83	3.7	39.69	2.84
<i>DE031</i>	14.13	52.53	Germany	Temperate	800	45	7	Autumn	11.89	76.53	7.18	1087.6	5.07	69.51	4.04
<i>DK018</i>	10.32	54.9	Denmark	Temperate	820	78	4	Summer	20.48	51.13	6.75	302.83	1.08	13.27	1.5
								Autumn	8.9	55.58	6.88	107.6	1.02	12.73	1.44
<i>DK034</i>	10.33	54.87	Denmark	Temperate	190	103	10	Autumn	7.7	71.39	7.54	507.02	21.39	14.59	3.48
<i>DK042</i>	10.35	54.87	Denmark	Temperate	645	100	12	Autumn	9.42	80.25	6.54	529.99	1.87	29.63	9.48





**Table A2. List of variables measured in this study, grouped by spacial scale: regional, landscape, local, sediment characteristics, dissolved organic matter and components of organic matter based on PARAFAC (Parallel Factor Analysis).**

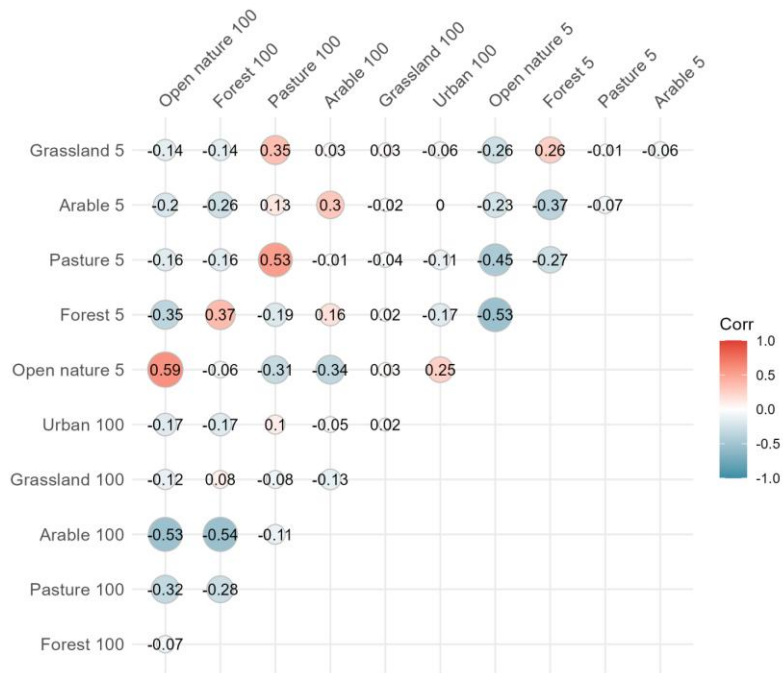
	Variable	Type	Unit
<b>Regional</b>	Temperature 40-year average (1978-2018)	Continuous	K
	Precipitation 40-year average (1978-2018)	Continuous	$\mu\text{m d}^{-1}$
	Climate	Categorical	(Mediterranean, Temperate)
	Annual temperature (2022)	Continuous	$^{\circ}\text{C}$
	Annual precipitation (2022)	Continuous	mm
	Latitude	Continuous	Decimal degrees (WGS 84)
<b>Landscape</b>	Open nature (5 m and 100)	Continuous	%
	Forest (5 m and 100)	Continuous	%
	Pasture (5 m and 100)	Continuous	%
	Arable (5 m and 100)	Continuous	%
	Grassland (5 m and 100)	Continuous	%
	Urban (5 m and 100)	Continuous	%
<b>Local pond characteristic</b>	ECELS index (Conservation status)	Continuous	0-100
	Coverage	Continuous	%
	PVI (plant volume inhabited)	Continuous	%
	Hydroperiod length	Continuous	months
	Area	Continuous	$\text{m}^2$
	Max depth	Continuous	cm
<b>Sediment characteristics</b>	Temperature	Continuous	$^{\circ}\text{C}$
	Water content	Continuous	%
	Organic matter	Continuous	%
	Carbonate content	Continuous	%
	pH	Continuous	
	Conductivity	Continuous	$\mu\text{S cm}^{-1}$
<b>Dissolved organic matter</b>	Texture	Categories	(Clay, Sandy, Loamy)
	Dissolved organic carbon (DOC)	Continuous	$\text{mg C g}^{-1}$
	Absorbance at 254 nm (Abs254)	Continuous	-
	Absorbance at 300 nm (Abs300)	Continuous	-
	BIX (biological index)	Continuous	-
	HIX (Humification index)	Continuous	-
<b>PARAFAC</b>	FI (fluorescence index)	Continuous	-
	SUVA	Continuous	$\text{L mg C}^{-1} \text{m}^{-1}$
	C1 Terrestrial humic-like	Continuous	-
	C2 Humic- like	Continuous	-
	C3 Tryptophan- like	Continuous	-



Appendix B: correlation among variables



Figure B1. Correlation matrix of environmental and sediment variables assessed in relation to CO<sub>2</sub> emissions in ponds. Pearson correlation coefficients (R) are displayed within the cells. The colour scale represents the strength and direction of the correlations, with red indicating positive and blue indicating negative relationships. Abbrev. C1 = terrestrial humic-like, C2 = humic-like and C3 = tryptophan-like.



480

**Figure B2. Correlation matrix of land use variables at 5m and 100m scales assessed in relation to CO<sub>2</sub> emissions in ponds. Pearson correlation coefficients (R) are shown within the matrix. The colour scale represents correlation strength and direction, with red indicating positive and blue indicating negative relationships.**

### Data availability

485 The datasets used in this study will be available, upon reasonable request.

### Author contribution

CT and SB conceived the study and helped supervise the project; VFA and CT developed the theory and performed the computations; VFA, LMP, CT, SB, PL, TB, and TD collected the field data; VFA, CT and LMP performed the laboratory analyses; RM supported the sediment analyses and provided material and infrastructure; TB and TD designed the CO<sub>2</sub> sensors and scripts for gas data collection; VFA analysed the data with support from CT, TB, and RM; VFA wrote the manuscript with substantial input from CT and SB; all authors revised, edited and approved the final version of the manuscript.

490



## Competing interests

495 The contact author has declared that none of the authors has any competing interests.

## Acknowledgements

We thank the PONDERFUL consortium; specially the staff off Aquatic Ecology Group (GEA) of the University of Vic - Central University of Catalonia, the GRECO research teams of the Institute of Aquatic Ecology of the University of Girona, the Aarhus University (AU), the Leibniz-Institute of Freshwater Ecology and Inland Fisheries (IGB), for assistance in the  
500 field and technical assistance. The authors acknowledge the use of the AI language model ChatGPT (OpenAI) to assist in improving the English language and writing style of this manuscript.

## Financial support

This research has received funding from the European Union's research and innovation programme (H2020) under grant agreement No 869296 – The PONDERFUL Project. SB, TAD, TB, and CT have also received funding from the  
505 MCIN/AEI/10.13039/501100011033/UE under the Biodiversa + TRANSPONDER grant (PCI2023-145983-2). VFA has a PhD fellowship from AGAUR-FI predoctoral program (2024 FI-3 00755) Joan Oró of the Secretariat of Universities and Research of the Department of Research and Universities of the Generalitat de Catalunya and the European Social Fund Plus. CT is a CONICET (Argentinean Council of Science) researcher. RM participated through the project Alter-C (Spanish Agencia Estatal de Investigación grant PID2020-114024GB-C32/AEI/10.13039/501100011033).

## 510 References

- Agnew, D., Fryirs, K. A., Ralph, T. J., and Kobayashi, T.: Soil carbon dynamics and aquatic metabolism of a wet–dry tropics wetland system, *Wetl Ecol Manag*, 29, 1–25, <https://doi.org/10.1007/s11273-020-09745-w>, 2021.
- Akaike, H.: Information Theory and an Extension of the Maximum Likelihood Principle, in: *Selected Papers of Hirotugu Akaike*, edited by: Parzen Emanuel and Tanabe, K. and K. G., Springer New York, New York, NY, 199–213,  
515 [https://doi.org/10.1007/978-1-4612-1694-0\\_15](https://doi.org/10.1007/978-1-4612-1694-0_15), 1998.
- Akasaka, M., Takamura, N., Mitsuhashi, H., and Kadono, Y.: Effects of land use on aquatic macrophyte diversity and water quality of ponds, *Freshw Biol*, 55, 909–922, <https://doi.org/10.1111/j.1365-2427.2009.02334.x>, 2010.
- Almeida, R., Paranaíba, J., Barbosa Alves, Í., Sobek, S., Kosten, S., Linkhorst, A., Mendonça, R., Quadra, G., Roland, F., and Barros, N.: Carbon dioxide emission from drawdown areas of a Brazilian reservoir is linked to surrounding land cover,  
520 *Aquat Sci*, 81, 68, <https://doi.org/10.1007/s00027-019-0665-9>, 2019.



- Baastrup-Spohr, L., Möller, C. L., and Sand-Jensen, K.: Water-level fluctuations affect sediment properties, carbon flux and growth of the isoetid *Littorella uniflora* in oligotrophic lakes, *Freshw Biol*, 61, 301–315, <https://doi.org/10.1111/fwb.12704>, 2016.
- Bartoń, K.: MuMIn: Multi-Model Inference, CRAN, [10.32614/CRAN.package.MuMIn](https://doi.org/10.32614/CRAN.package.MuMIn), 2023.
- 525 Bartrons, M., Yang, J., Cuenca Cambronero, M., Lemmens, P., Anton-Pardo, M., Beklioglu, M., Biggs, J., Boissezon, A., Boix, D., Calvo, C., Colina, M., Davidson, T. A., De Meester, L., Fahy, J. C., Greaves, H. M., Kiran Isufi, H., Levi, E. E., Meerhoff, M., Mehner, T., Mülâyim, E. B., Oertli, B., Patmore, I. R., Sayer, C. D., Villà-Freixa, J., and Brucet, S.: Why ponds concentrate nutrients: the roles of internal features, land use, and climate, *Hydrobiologia*, <https://doi.org/10.1007/s10750-025-05907-0>, 2025.
- 530 Bastviken, D., Sundgren, I., Natchimuthu, S., Reyier, H., and Gålfalk, M.: Technical Note: Cost-efficient approaches to measure carbon dioxide (CO<sub>2</sub>) fluxes and concentrations in terrestrial and aquatic environments using mini loggers, *Biogeosciences*, 12, 3849–3859, <https://doi.org/10.5194/bg-12-3849-2015>, 2015.
- Beringer, J., Livesley, S. J., Randle, J., and Hutley, L. B.: Carbon dioxide fluxes dominate the greenhouse gas exchanges of a seasonal wetland in the wet-dry tropics of Northern Australia, *Agric For Meteorol*, 182–183, 239–247, <https://doi.org/10.1016/j.agrformet.2013.06.008>, 2013.
- 535 Bevacqua, E., Rakovec, O., Schumacher, D. L., Kumar, R., Thober, S., Samaniego, L., Seneviratne, S. I., and Zscheischler, J.: Direct and lagged climate change effects intensified the 2022 European drought, *Nat Geosci*, 17, 1100–1107, <https://doi.org/10.1038/s41561-024-01559-2>, 2024.
- Bhushan, A., Goyal, V. C., and Srivastav, A. L.: Greenhouse gas emissions from inland water bodies and their rejuvenation: a review, *J. Water Clim. Chang*, 15, 5626–5644, <https://doi.org/10.2166/wcc.2024.561>, 2024.
- 540 Bolker, B. M., Brooks, M. E., Clark, C. J., Geange, S. W., Poulsen, J. R., Stevens, M. H. H., and White, J. S. S.: Generalized linear mixed models: a practical guide for ecology and evolution, *Trends Ecol. Evol*, 24, 127–135, <https://doi.org/10.1016/j.tree.2008.10.008>, 2009.
- Bottino, F., Souza, B. P., Rocha, R. J. S., Cunha-Santino, M. B., and Bianchini, I.: Characterization of humic substances from five macrophyte species decomposed under different nutrient conditions, *Limnetica*, 40, 267–278, <https://doi.org/10.23818/limn.40.18>, 2021.
- 545 Buragienė, S., Šarauskis, E., Romanekas, K., Adamavičienė, A., Kriaučiūnienė, Z., Avižienytė, D., Marozas, V., and Naujokienė, V.: Relationship between CO<sub>2</sub> emissions and soil properties of differently tilled soils, *Sci. Total Environ.*, 662, 786–795, <https://doi.org/10.1016/j.scitotenv.2019.01.236>, 2019.
- 550 Burkett, V. and Kusler, J.: Climate change: Potential impacts and interactions in wetlands of the United States, *J Am Water Resour Assoc*, 36, 313–320, <https://doi.org/10.1111/j.1752-1688.2000.tb04270.x>, 2000.
- Catalán, N., Von Schiller, D., Marcé, R., Koschorreck, M., Gomez-Gener, L., and Obrador, B.: Carbon dioxide efflux during the flooding phase of temporary ponds, *Limnetica*, 29, 349–360, <http://doi.org/10.23818/limn.33.27>, 2014.



- Čížková, H., Květ, J., Comín, F. A., Laiho, R., Pokorný, J., and Pithart, D.: Actual state of European wetlands and their possible future in the context of global climate change, *Aquat Sci*, 75, 3–26, <https://doi.org/10.1007/s00027-011-0233-4>, 2013.
- Cole, J. J. and Caraco, N. F.: Atmospheric exchange of carbon dioxide in a low-wind oligotrophic lake measured by the addition of SF<sub>6</sub>, *Limnol Oceanogr*, 43, 647–656, <https://doi.org/10.4319/lo.1998.43.4.0647>, 1998.
- Cole, J. J., Prairie, Y. T., Caraco, N. F., McDowell, W. H., Tranvik, L. J., Striegl, R. G., Duarte, C. M., Kortelainen, P., Downing, J. A., Middelburg, J. J., and Melack, J.: Plumbing the global carbon cycle: Integrating inland waters into the terrestrial carbon budget, *Ecosystems*, 10, 171–184, <https://doi.org/10.1007/s10021-006-9013-8>, 2007.
- Copernicus Climate Change Service (C3S): European State of the Climate 2022, Copernicus Climate Change Service, <https://climate.copernicus.eu/ESOTC/2022>, 2023.
- DelVecchia, A. G., Gougherty, S., Taylor, B. W., and Wissinger, S. A.: Biogeochemical characteristics and hydroperiod affect carbon dioxide flux rates from exposed high-elevation pond sediments, *Limnol Oceanogr*, 66, 1050–1067, <https://doi.org/10.1002/lno.11663>, 2021.
- Dimitriou, E., Moussoulis, E., Stamati, F., and Nikolaidis, N.: Modelling hydrological characteristics of Mediterranean Temporary Ponds and potential impacts from climate change, *Hydrobiologia*, 634, 195–208, <https://doi.org/10.1007/s10750-009-9898-2>, 2009.
- Douglas Bates, Martin Mächler, Ben Bolker, and Steve Walker: Fitting Linear Mixed-Effects Models Using lme4, *J Stat Softw*, 67, 1–48, <https://doi.org/10.18637/jss.v067.i01>, 2015.
- Downing, J. A.: Emerging global role of small lakes and ponds: Little things mean a lot, *Limnetica*, 29, 9–24, <https://doi.org/10.23818/limn.29.02>, 2010.
- Fellman, J., Hood, E., and Spencer, R.: Fluorescence spectroscopy opens new windows into dissolved organic matter dynamics in freshwater ecosystems: A review, *Limnol Oceanogr*, 55, 2452–2462, <https://doi.org/10.4319/lo.2010.55.6.2452>, 2010.
- Fox, J.: Effect Displays in R for Generalised Linear Models, *J Stat Softw*, 8, 1–27, <https://doi.org/10.18637/jss.v008.i15>, 2003.
- Fraser, F. C., Corstanje, R., Deeks, L. K., Harris, J. A., Pawlett, M., Todman, L. C., Whitmore, A. P., and Ritz, K.: On the origin of carbon dioxide released from rewetted soils, *Soil Biol Biochem*, 101, 1–5, <https://doi.org/10.1016/j.soilbio.2016.06.032>, 2016.
- Fromin, N., Pinay, G., Montuelle, B., Landais, D., Ourcival, J. M., Joffre, R., and Lensi, R.: Impact of seasonal sediment desiccation and rewetting on microbial processes involved in greenhouse gas emissions, *Ecohydrology*, 3, 339–348, <https://doi.org/10.1002/eco.115>, 2010.
- Gabor, R., Baker, A., Mcknight, D., and Miller, M.: Fluorescence Indices and Their Interpretation, in: *Aquatic Organic Matter Fluorescence*, edited by: Coble, P. G., Lead, J., Baker, A., Reynolds, D. M., and Spencer, R. G. M., Cambridge University Press, Cambridge, 303–338, <https://doi.org/10.1017/CBO9781139045452.015>, 2014.



- Gao, Y., Li, J., Wang, S., Jia, J., Wu, F., and Yu, G.: Global inland water greenhouse gas (GHG) geographical patterns and escape mechanisms under different water level, *Water Res.*, 269, 122808, <https://doi.org/10.1016/j.watres.2024.122808>, 2025.
- Garcia-Murillo, P., Díaz-Paniagua, C., and Fernández-Zamudio, R.: Decline of aquatic plants in an iconic European protected natural area, *J Nat Conserv*, 84, 126814, <https://doi.org/10.1016/j.jnc.2024.126814>, 2025.
- Gilbert, P. J., Cooke, D. A., Deary, M., Taylor, S., and Jeffries, M. J.: Quantifying rapid spatial and temporal variations of CO<sub>2</sub> fluxes from small, lowland freshwater ponds, *Hydrobiologia*, 793, 83–93, <https://doi.org/10.1007/s10750-016-2855-y>, 2017.
- Gómez-Gener, L., Obrador, B., Marcé, R., Acuña, V., Catalán, N., Casas-Ruiz, J. P., Sabater, S., Muñoz, I., and von Schiller, D.: When Water Vanishes: Magnitude and Regulation of Carbon Dioxide Emissions from Dry Temporary Streams, *Ecosystems*, 19, 710–723, <https://doi.org/10.1007/s10021-016-9963-4>, 2016.
- Gómez-Rodríguez, C., Bustamante, J., and Díaz-Paniagua, C.: Evidence of hydroperiod shortening in a preserved system of temporary ponds, *Remote Sens*, 2, 1439–1462, <https://doi.org/10.3390/rs2061439>, 2010.
- Google LLC: Google Earth Pro, <https://www.google.com/earth/>, 2021.
- Sen Gupta, R. and Koroleff, F.: A quantitative study of nutrient fractions and a stoichiometric model of the Baltic, *Estuar. Coast. Shelf Sci.*, 1, 335–360, [https://doi.org/10.1016/0302-3524\(73\)90025-X](https://doi.org/10.1016/0302-3524(73)90025-X), 1973.
- Håkanson, L.: On the relationship between lake trophic level and lake sediments, *Water Res.*, 18, 303–314, [https://doi.org/https://doi.org/10.1016/0043-1354\(84\)90104-0](https://doi.org/https://doi.org/10.1016/0043-1354(84)90104-0), 1984.
- Hanken, N.-M., Bjørlykke, K., and Nielsen, J. K.: Carbonate Sediments, in: *Petroleum Geoscience: From Sedimentary Environments to Rock Physics*, edited by: Bjørlykke, K., Springer Berlin Heidelberg, Berlin, Heidelberg, 151–216, [https://doi.org/10.1007/978-3-642-34132-8\\_5](https://doi.org/10.1007/978-3-642-34132-8_5), 2015.
- Hanson, P. C., Pace, M. L., Carpenter, S. R., Cole, J. J., and Stanley, E. H.: Integrating Landscape Carbon Cycling: Research Needs for Resolving Organic Carbon Budgets of Lakes, *Ecosystems*, 18, 363–375, <https://doi.org/10.1007/s10021-014-9826-9>, 2015.
- Hartig, F.: DHARMA: Residual Diagnostics for Hierarchical (Multi-Level / Mixed) Regression Models, 2022.
- Hill, M. J., Greaves, H. M., Sayer, C. D., Hassall, C., Milin, M., Milner, V. S., Marazzi, L., Hall, R., Harper, L. R., Thornhill, I., Walton, R., Biggs, J., Ewald, N., Law, A., Willby, N., White, J. C., Briers, R. A., Mathers, K. L., Jeffries, M. J., and Wood, P. J.: Pond ecology and conservation: research priorities and knowledge gaps, *Ecosphere*, 12, <https://doi.org/10.1002/ecs2.3853>, 2021.
- Holgerson, M. A. and Raymond, P. A.: Large contribution to inland water CO<sub>2</sub> and CH<sub>4</sub> emissions from very small ponds, *Nat Geosci*, 9, 222–226, <https://doi.org/10.1038/ngeo2654>, 2016.
- Huguet, A., Vacher, L., Relexans, S., Saubusse, S., Froidefond, J. M., and Parlanti, E.: Properties of fluorescent dissolved organic matter in the Gironde Estuary, *Org Geochem*, 40, 706–719, <https://doi.org/https://doi.org/10.1016/j.orggeochem.2009.03.002>, 2009.





- IPCC: Climate change 2014: synthesis report, edited by: Contribution of working Groups I, II and III to the fifth assessment report of the I. P. on C. C., Geneva, 2014.
- Jarvis, P., Petsikos, C., Wingate, L., Rayment, M., Pereira, J., Banza, J., David, J., Miglietta, F., Borghetti, M., Manca, G.,  
625 and Valentini, R.: Drying and wetting of Mediterranean soils stimulates decomposition and carbon dioxide emission: The  
“Birch effect,” *Tree Physiol*, 27, 929–940, <https://doi.org/10.1093/treephys/27.7.929>, 2007.
- Keller, P. S., Catalán, N., von Schiller, D., Grossart, H. P., Koschorreck, M., Obrador, B., Frassl, M. A., Karakaya, N.,  
Barros, N., Howitt, J. A., Mendoza-Lera, C., Pastor, A., Flaim, G., Aben, R., Riis, T., Arce, M. I., Onandia, G., Paranaíba, J.  
R., Linkhorst, A., del Campo, R., Amado, A. M., Cauvy-Fraunié, S., Brothers, S., Condon, J., Mendonça, R. F., Reverey, F.,  
630 Rõõm, E. I., Datry, T., Roland, F., Laas, A., Obertegger, U., Park, J. H., Wang, H., Kosten, S., Gómez, R., Feijoó, C.,  
Elosegi, A., Sánchez-Montoya, M. M., Finlayson, C. M., Melita, M., Oliveira Junior, E. S., Muniz, C. C., Gómez-Gener, L.,  
Leigh, C., Zhang, Q., and Marcé, R.: Global CO<sub>2</sub> emissions from dry inland waters share common drivers across  
ecosystems, *Nat Commun*, 11, <https://doi.org/10.1038/s41467-020-15929-y>, 2020.
- Lauerwald, R., Allen, G. H., Deemer, B. R., Liu, S., Maavara, T., Raymond, P., Alcott, L., Bastviken, D., Hastie, A.,  
635 Holgerson, M. A., Johnson, M. S., Lehner, B., Lin, P., Marzadri, A., Ran, L., Tian, H., Yang, X., Yao, Y., and Regnier, P.:  
Inland Water Greenhouse Gas Budgets for RECCAP2: 2. Regionalization and Homogenization of Estimates, *Global  
Biogeochem Cycles*, 37, <https://doi.org/10.1029/2022GB007658>, 2023.
- Lee, S.-Y., Ryan, M. E., Hamlet, A. F., Palen, W. J., Lawler, J. J., and Halabisky, M.: Projecting the Hydrologic Impacts of  
Climate Change on Montane Wetlands, *PLoS One*, 10, e0136385-, <https://doi.org/10.1371/journal.pone.0136385>, 2015.
- 640 Lellei-Kovács, E., Kovács-Láng, E., Botta-Dukát, Z., Kalapos, T., Emmett, B., and Beier, C.: Thresholds and interactive  
effects of soil moisture on the temperature response of soil respiration, *Eur J Soil Biol*, 47, 247–255,  
<https://doi.org/10.1016/j.ejsobi.2011.05.004>, 2011.
- Lenth, R. V.: emmeans: Estimated Marginal Means, aka Least-Squares Means, R package, 2025.
- Lloyd, J. and Taylor, J. A.: On the Temperature Dependence of Soil Respiration, *Funct Ecol*, 8, 315–323,  
645 <https://doi.org/10.2307/2389824>, 1994.
- López-de Sancha, A., Benejam, L., Boix, D., Briggs, L., Cuenca-Cambronero, M., Davidson, T. A., De Meester, L., Fahy, J.  
C., Lemmens, P., Martin, B., Mehner, T., Oertli, B., Rasmussen, M., Greaves, H. M., Sayer, C., Beklioglu, M., Brys, R., and  
Brucet, S.: Drivers of amphibian species richness in European ponds, *Ecography*, <https://doi.org/10.1111/ecog.07347>, 2025a.
- López-de Sancha, Alejandro., Boix, D., Benejam, L., Briggs, L., Davidson, T. A., Fahy, J. C., Frutos-Aragón, V., Greaves,  
650 H. M., Lemmens, P., Mehner, T., Martín, L., Oertli, B., Sayer, C., and Brucet, S.: Amphibian conservation in Europe: the  
importance of pond condition, *Biodivers Conserv*, <https://doi.org/10.1007/s10531-025-03033-w>, 2025b.
- Marcé, R., Obrador, B., Gómez-Gener, L., Catalán, N., Koschorreck, M., Arce, M. I., Singer, G., and von Schiller, D.:  
Emissions from dry inland waters are a blind spot in the global carbon cycle, <https://doi.org/10.1016/j.earscirev.2018.11.012>,  
2019.



- 655 Martinsen, K. T., Kragh, T., and Sand-Jensen, K.: Carbon dioxide fluxes of air-exposed sediments and desiccating ponds, *Biogeochemistry*, 144, 165–180, <https://doi.org/10.1007/s10533-019-00579-0>, 2019.
- Morant, D., Picazo, A., Rochera, C., Santamans, A. C., Miralles-Lorenzo, J., and Camacho, A.: Influence of the conservation status on carbon balances of semiarid coastal Mediterranean wetlands, *Inland Waters*, 10, 453–467, <https://doi.org/10.1080/20442041.2020.1772033>, 2020.
- 660 Murphy, K. R., Stedmon, C. A., Graeber, D., and Bro, R.: Fluorescence spectroscopy and multi-way techniques. PARAFAC, *Anal. Methods*, 5, 6557, <https://doi.org/10.1039/c3ay41160e>, 2013.
- Nag, S. K., Das Ghosh, B., Nandy, S., Aftabuddin, M., Sarkar, U. K., and Das, B. K.: Comparative assessment of carbon sequestration potential of different types of wetlands in lower Gangetic basin of West Bengal, India, *Environ Monit Assess*, 195, 154, <https://doi.org/10.1007/s10661-022-10729-x>, 2023.
- 665 Novikmec, M., Hamerlík, L., Kočícký, D., Hrivnák, R., Kochjarová, J., O’ahel’ová, H., Pa’ove-Balang, P., and Svitok, M.: Ponds and their catchments: size relationships and influence of land use across multiple spatial scales, *Hydrobiologia*, 774, 155–166, <https://doi.org/10.1007/s10750-015-2514-8>, 2016.
- Obrador, B., Von Schiller, D., Marcé, R., Gómez-Gener, L., Koschorreck, M., Borrego, C., and Catalán, N.: Dry habitats sustain high CO<sub>2</sub> emissions from temporary ponds across seasons, *Sci Rep*, 8, 3015, [https://doi.org/10.1038/s41598-018-](https://doi.org/10.1038/s41598-018-20969-y)
- 670 [20969-y](https://doi.org/10.1038/s41598-018-20969-y), 2018.
- Oertel, C., Matschullat, J., Zurba, K., Zimmermann, F., and Erasmi, S.: Greenhouse gas emissions from soils—A review, *Chem. Erde*, 76, 327–352, <https://doi.org/10.1016/j.chemer.2016.04.002>, 2016.
- Oertli, B., Céréghino, R., Hull, A., and Miracle, R.: Pond conservation: From science to practice, *Hydrobiologia*, 634, 1–9, <https://doi.org/10.1007/s10750-009-9891-9>, 2009.
- 675 Oroud, I. M.: The implications of climate change on freshwater resources in the arid and semiarid Mediterranean environments using hydrological modeling, GIS tools, and remote sensing, *Environ Monit Assess*, 196, 979, <https://doi.org/10.1007/s10661-024-13139-3>, 2024.
- Page, K. L. and Dalal, R. C.: Contribution of natural and drained wetland systems to carbon stocks, CO<sub>2</sub>, N<sub>2</sub>O, and CH<sub>4</sub> fluxes: An Australian perspective, *Soil Res.*, 49, 377–388, <https://doi.org/10.1071/SR11024>, 2011.
- 680 Pekel, J.-F., Cottam, A., Gorelick, N., and Belward, A. S.: High-resolution mapping of global surface water and its long-term changes, *Nature*, 540, 418–422, <https://doi.org/10.1038/nature20584>, 2016.
- Petersen, S. O., Hoffmann, C. C., Schäfer, C. M., Blicher-Mathiesen, G., Elsgaard, L., Kristensen, K., Larsen, S. E., Torp, S. B., and Greve, M. H.: Annual emissions of CH<sub>4</sub> and N<sub>2</sub>O, and ecosystem respiration, from eight organic soils in Western Denmark managed by agriculture, *Biogeosciences*, 9, 403–422, <https://doi.org/10.5194/bg-9-403-2012>, 2012.
- 685 Peterson, R. A. and Cavanaugh, J. E.: Ordered quantile normalization: a semiparametric transformation built for the cross-validation era, *J Appl Stat*, 47, 2312–2327, <https://doi.org/10.1080/02664763.2019.1630372>, 2020.



- Pickens, A. H., Hansen, M. C., Hancher, M., Stehman, S. V., Tyukavina, A., Potapov, P., Marroquin, B., and Sherani, Z.: Mapping and sampling to characterize global inland water dynamics from 1999 to 2018 with full Landsat time-series, *Remote Sens Environ*, 243, 111792, <https://doi.org/10.1016/j.rse.2020.111792>, 2020.
- 690 Pozzo-Pirotta, L. J., Montes-Pérez, J. J., Sammartino, S., Marcé, R., Obrador, B., Escot, C., Reyes, I., and Moreno-Ostos, E.: Carbon dioxide emission from drawdown areas of a Mediterranean reservoir, *Limnetica*, 41, 61–72, <https://doi.org/10.23818/limn.41.05>, 2022.
- Prananto, J. A., Minasny, B., Comeau, L. P., Rudiyanto, R., and Grace, P.: Drainage increases CO<sub>2</sub> and N<sub>2</sub>O emissions from tropical peat soils, *Glob Chang Biol*, 26, 4583–4600, <https://doi.org/10.1111/gcb.15147>, 2020.
- 695 Premke, K., Attermeyer, K., Augustin, J., Cabezas, A., Casper, P., Deumlich, D., Gelbrecht, J., Gerke, H. H., Gessler, A., Grossart, H. P., Hilt, S., Hupfer, M., Kalettka, T., Kayler, Z., Lischeid, G., Sommer, M., and Zak, D.: The importance of landscape diversity for carbon fluxes at the landscape level: small-scale heterogeneity matters, *Wiley Interdisciplinary Reviews: Water*, 3, 601–617, <https://doi.org/10.1002/wat2.1147>, 2016.
- Pucher, M., Wünsch, U., Weigelhofer, G., Murphy, K., Hein, T., and Graeber, D.: StaRdom: Versatile software for analyzing spectroscopic data of dissolved organic matter in R, *Water*, 11, 2366, <https://doi.org/10.3390/w11112366>, 2019.
- 700 R Core Team: R: A language and environment for statistical computing, R Foundation for Statistical Computing, Vienna, Austria, <https://www.R-project.org/>, 2024.
- Raymond, P. A., Hartmann, J., Lauerwald, R., Sobek, S., McDonald, C., Hoover, M., Butman, D., Striegl, R., Mayorga, E., Humborg, C., Kortelainen, P., Dürr, H., Meybeck, M., Ciais, P., and Guth, P.: Global carbon dioxide emissions from inland waters, *Nature*, 503, 355–359, <https://doi.org/10.1038/nature12760>, 2013.
- 705 Rey, A.: Mind the gap: Non-biological processes contributing to soil CO<sub>2</sub> efflux, *Glob. Change Biol.*, 21, 1752–1761, <https://doi.org/10.1111/gcb.12821>, 2015.
- Roland, M., Serrano-Ortiz, P., Kowalski, A. S., Goddérís, Y., Sánchez-Cañete, E. P., Ciais, P., Domingo, F., Cuezva, S., Sanchez-Moral, S., Longdoz, B., Yakir, D., Van Grieken, R., Schott, J., Cardell, C., and Janssens, I. A.: Atmospheric turbulence triggers pronounced diel pattern in karst carbonate geochemistry, *Biogeosciences*, 10, 5009–5017, <https://doi.org/10.5194/bg-10-5009-2013>, 2013.
- Rulík, M., Weber, L., Min, S., and Šmíd, R.: CO<sub>2</sub> and CH<sub>4</sub> fluxes from inundated floodplain ponds: role of diel variability and duration of inundation, *Front Environ Sci*, 11, <https://doi.org/10.3389/fenvs.2023.1006988>, 2023.
- Ryan A. Peterson: Finding Optimal Normalizing Transformations via bestNormalize, *R J*, 13, 310–329, <https://doi.org/10.32614/RJ-2021-041>, 2021.
- 715 Sabater, S., Timoner, X., Borrego, C., and Acuña, V.: Stream biofilm responses to flow intermittency: From cells to ecosystems, *Front Environ Sci*, 4, <https://doi.org/10.3389/fenvs.2016.00014>, 2016.
- Sala, J., Gascón, S., Boix, D., Gestí, J., and Quintana, X. D.: Proposal of a rapid methodology to assess the conservation status of Mediterranean wetlands and its application in Catalunya (NE Iberian Peninsula), *Arch. Sci.*, 57, 123–132, 2005.



- 720 Sánchez-Carrillo, S.: Hydrology and biogeochemistry of Mediterranean temporary ponds, International Conference on Mediterranean Temporary Ponds. Proceedings and Abstracts, 73–82, 2009.
- Sponseller, R. A.: Precipitation pulses and soil CO<sub>2</sub> flux in a Sonoran Desert ecosystem, *Glob Chang Biol*, 13, 426–436, <https://doi.org/https://doi.org/10.1111/j.1365-2486.2006.01307.x>, 2007.
- Suh, S., Lee, E., and Lee, J.: Temperature and moisture sensitivities of CO<sub>2</sub> efflux from lowland and alpine meadow soils, 725 *Journal of Plant Ecology*, 2, 225–231, <https://doi.org/10.1093/jpe/rtp021>, 2009.
- Tak, D. B. Y., Vroom, R. J. E., Lexmond, R., Lamers, L. P. M., Robroek, B. J. M., and Temmink, R. J. M.: Water level and vegetation type control carbon fluxes in a newly-constructed soft-sediment wetland, *Wetl Ecol Manag*, 31, 583–594, <https://doi.org/10.1007/s11273-023-09936-1>, 2023.
- Taylor, S., Gilbert, P. J., Cooke, D. A., Deary, M. E., and Jeffries, M. J.: High carbon burial rates by small ponds in the 730 landscape, *Front Ecol Environ*, 17, 25–31, <https://doi.org/10.1002/fee.1988>, 2019.
- Thien, S. J.: A flow diagram for teaching texture-by-feel analysis, *Journal of Agronomic Education*, 8, 54–55, <https://doi.org/https://doi.org/10.2134/jae.1979.0054>, 1979.
- Tranvik, L. J., Downing, J. A., Cotner, J. B., Loiselle, S. A., Striegl, R. G., Ballatore, T. J., Dillon, P., Finlay, K., Fortino, K., Knoll, L. B., Kortelainen, P. L., Kutser, T., Larsen, Soren., Laurion, I., Leech, D. M., McCallister, S. L., McKnight, D. M., 735 Melack, J. M., Overholt, E., Porter, J. A., Prairie, Y., Renwick, W. H., Roland, F., Sherman, B. S., Schindler, D. W., Sobek, S., Tremblay, A., Vanni, M. J., Verschoor, A. M., von Wachenfeldt, E., and Weyhenmeyer, G. A.: Lakes and reservoirs as regulators of carbon cycling and climate, *Limnol Oceanogr*, 54, 2298–2314, [https://doi.org/https://doi.org/10.4319/lo.2009.54.6\\_part\\_2.2298](https://doi.org/https://doi.org/10.4319/lo.2009.54.6_part_2.2298), 2009.
- Unger, S., Máguas, C., Pereira, J. S., David, T. S., and Werner, C.: The influence of precipitation pulses on soil respiration - 740 Assessing the “Birch effect” by stable carbon isotopes, *Soil Biol Biochem*, 42, 1800–1810, <https://doi.org/10.1016/j.soilbio.2010.06.019>, 2010.
- Verpoorter, C., Kutser, T., Seekell, D. A., and Tranvik, L. J.: A global inventory of lakes based on high-resolution satellite imagery, *Geophys Res Lett*, 41, 6396–6402, <https://doi.org/10.1002/2014GL060641>, 2014.
- Vicente-Serrano, S. M., Peña-Angulo, D., Beguería, S., Domínguez-Castro, F., Tomás-Burguera, M., Noguera, I., Gimeno- 745 Sotelo, L., and El Kenawy, A.: Global drought trends and future projections, *Philosophical Transactions of the Royal Society A: Mathematical, Physical and Engineering Sciences*, 380, 20210285, <https://doi.org/10.1098/rsta.2021.0285>, , 2022.
- Voudouri, M. O., Liaskou, P., Manios, E. M., and Anagnostopoulou, C.: Top European Droughts since 1991, 94, <https://doi.org/10.3390/environsciproc2023026094>, 2023.
- Wang, J., Song, C., Reager, J. T., Yao, F., Famiglietti, J. S., Sheng, Y., MacDonald, G. M., Brun, F., Schmied, H. M., 750 Marston, R. A., and Wada, Y.: Recent global decline in endorheic basin water storages, *Nat Geosci*, 11, 926–932, <https://doi.org/10.1038/s41561-018-0265-7>, 2018.



- Wang, M., Hao, T., Deng, X., Wang, Z., Cai, Z., and Li, Z.: Effects of sediment-borne nutrient and litter quality on macrophyte decomposition and nutrient release, *Hydrobiologia*, 787, 205–215, <https://doi.org/10.1007/s10750-016-2961-x>, 2017.
- 755 Wei, T. and Simko, V.: R package “corrplot”: Visualization of a Correlation Matrix, GitHub, <https://github.com/taiyun/corrplot>, 2024.
- Weisberg, S. and Fox, J.: *Multivariate Linear Models in R*, in: *An R Companion to Applied Regression*, Sage, Thousand Oaks, CA, 2011.
- Weise, L., Ulrich, A., Moreano, M., Gessler, A., E. Kayler, Z., Steger, K., Zeller, B., Rudolph, K., Knezevic-Jaric, J., and  
760 Premke, K.: Water level changes affect carbon turnover and microbial community composition in lake sediments, *FEMS Microbiol Ecol*, 92, fiw035, <https://doi.org/10.1093/femsec/fiw035>, 2016.
- Weishaar, J. L., Aiken, G. R., Bergamaschi, B. A., Fram, M. S., Fujii, R., and Mopper, K.: Evaluation of Specific Ultraviolet Absorbance as an Indicator of the Chemical Composition and Reactivity of Dissolved Organic Carbon, *Environ Sci Technol*, 37, 4702–4708, <https://doi.org/10.1021/es030360x>, 2003.
- 765 Wickham, H.: *ggplot2: Elegant Graphics for Data Analysis*, 2nd Edn., Springer, Cham, <https://doi.org/10.1007/978-3-319-24277-4>, 2016.
- Williams, A., Williams, P., Biggs, J., Fox, G., Nicolet, P., Whitfield Williams, M. P., Biggs, J., Fox, G., Nicolet, P., and Whitfield, M.: History, origins and importance of temporary ponds Item Type article History, Origins And Importance Of Temporary Ponds, *Freshwater Forum*, 17, 1–10, 2010.
- 770 Wouters, H.: Downscaled bioclimatic indicators for selected regions from 1978 to 2018 derived from reanalysis, Copernicus Climate Data Store (CDS) , ERA5, <https://cds.climate.copernicus.eu/datasets/sis-biodiversity-era5-regional>, accessed on 01-Jun-2023, 2021.
- Zhao, M., Han, G., Li, J., Song, W., Qu, W., Eller, F., Wang, J., and Jiang, C.: Responses of soil CO<sub>2</sub> and CH<sub>4</sub> emissions to changing water table level in a coastal wetland, *J Clean Prod*, 269, 122316, <https://doi.org/10.1016/j.jclepro.2020.122316>,  
775 2020.
- Zou, J., Ziegler, A. D., Chen, D., McNicol, G., Ciais, P., Jiang, X., Zheng, C., Wu, J., Wu, J., Lin, Z., He, X., Brown, L. E., Holden, J., Zhang, Z., Ramchunder, S. J., Chen, A., and Zeng, Z.: Rewetting global wetlands effectively reduces major greenhouse gas emissions, *Nat Geosci*, 15, 627–632, <https://doi.org/10.1038/s41561-022-00989-0>, 2022.